Hindawi
International Journal of Aerospace Engineering
Volume 2020, Article ID 2069631, 17 pages
https://doi.org/10.1155/2020/2069631

Research Article

Distance-Based Formation Control for Quadrotors with Collision Avoidance via Lyapunov Barrier Functions

Jawhar Ghommam,[1] **Luis F. Luque-Vega**,[2] **and Maarouf Saad**[3]

[1]*Department of Electrical and Computer Engineering, College of Engineering, Sultan Qaboos University, Oman*
[2]*Centro de Investigación, Innovación y Desarrollo Tecnológico CIIDETEC-UVM, Universidad del Valle de México, Tlaquepaque, Jalisco 45601, Mexico*
[3]*Department of Electrical Engineering, École de Technologie Superieure, Montréal, QC, Canada*

Correspondence should be addressed to Jawhar Ghommam; jawher@squ.edu.om

Received 11 December 2019; Revised 14 March 2020; Accepted 24 June 2020; Published 20 July 2020

Academic Editor: Jacopo Serafini

In this paper, group formation control with collision avoidance is investigated for heterogeneous multiquadrotor vehicles. Specifically, the distance-based formation and tracking control problem are addressed in the framework of leader-follower architecture. In this scheme, the leader is assigned the task of intercepting a target whose velocity is unknown, while the follower quadrotors are arranged to set up a predefined rigid formation pattern, ensuring simultaneously interagent collision avoidance and relative localization. The adopted strategy for the control design consists in decoupling the quadrotor dynamics in a cascaded structure to handle its underactuated property. Furthermore, by imposing constraints on the orientation angles, the follower will never be overturned. Rigorous stability analysis is presented to prove the stability of the entire closed-loop system. Numerical simulation results are presented to validate the proposed control strategy.

1. Introduction

1.1. Background and Related Works. Quadrotors are agile mechanical systems which have drawn the attention of researchers for the last decades [1–3], mainly because the use of these types of aerial vehicles is appealing for several real-world applications. Due to their excellent performances, quadrotors are likely to be adopted in various civil potential applications such as inspection of power lines, oil platforms, search and rescue operations, and surveillance [4, 5]. On the other hand, it is worth pointing out that a team of quadrotors has many benefits over using a single quadrotor in several applications where it results in faster and more efficient operations. The coordination of multiple quadrotors to perform cooperative tasks has received considerable attention due to the challenges arising in their control design. Coordinated movement of quadrotors comes with several methodologies and approaches proposed over the last few years [6–10]. From the control structure perspective, the approaches used for coordinated control can be categorized into centralized and decentralized methods. In the centralized method, the control signals for all the agents are generated in the leader agent or in a central station [7, 11]. Whereas, in the decentralized method also known as the distributed method, each member of the team uses its own local controller enhanced with local information from its close neighbors [6, 8, 10].

From the control mechanism perspective, there are roughly five approaches to cooperative control of multiple aerial vehicles: the behavioral-based approach [12, 13] where each agent locally reacts to actions of its neighbors. This method is categorized under the decentralized approach and is suitable for a large number of agents in the group. The disadvantage of this approach, however, is that the complexity of the dynamics of the group of robots cannot be amenable to mathematical stability analysis. Another important approach is the virtual structure approach [14–17]. This approach considers all the agents in the group as a single entity, thus limiting the formation scenarios that can be anticipated to merely static formation patterns. Moreover, the priority of agents in the group team is to respect one

of the two rules: following their individual trajectories [18] or maintaining the group formation. The artificial potential function-based approach [6, 19, 20] is a powerful tool as it allows the agents to evolve in a cohesive motion while avoiding obstacles. The disadvantage of this approach is that local minima may appear where the vector field vanishes, therefore forcing the agents to get trapped into undesired equilibrium points. The leader-following approach [11, 21, 22], on the other hand, seems to be particularly attractive and preferred over the aforementioned approaches due to its simplicity and scalability. In this approach, some agents are designated as leaders aimed at tracking predefined trajectories, while others are treated as followers whose actions are merely to follow the leader(s) in order to keep the formation. The followers can in turn be designated as leaders for other vehicles in the group resulting in a scalability of the formation. The advantage of this approach is that from the definition of the motion of one entity, the overall group behavior can subsequently be defined. Also, it should be pointed out that the internal formation stability is induced by the control laws of individual vehicles. A major drawback of this approach, however, is that there exists no feedback from the followers to the leaders. Consequently, if the followers are perturbed, the coordination shape of the group team cannot be maintained.

A leader-follower formation control algorithm for multi-quadrotors was proposed in [22, 23] that involves a linear inner-loop and nonlinear outer-loop control structure, where a combination of sliding mode control and LQR/PD technique was deployed for the trajectory tracking control of a follower to track a leader quadrotor. The formation shape is formed then maintained by keeping a constant distance and a desired angle between each follower and the leader. The authors in [24] proposed a control strategy for a string-like formation of multiple autonomous quadrotor vehicles. In this approach, the objective is to design a maneuvering control for the quadrotor group along a geometric path while respecting an assigned timing law that determines the formation rate of advancement. A formation control strategy has been proposed [11] using the leader-follower approach. The suggested approach differs from common strategies employed for leader-follower schemes and consists in stabilizing, at a predefined distance vector, the position of the leader in the body frame of a virtual follower which in turn generates a trajectory which is used as a reference trajectory to be tracked by the real follower vehicle. The proposed strategy allows for generating curvature-rich formation trajectories. The authors in [25] proposed a 3D leader-follower formation control strategy for a quadrotor with completely unknown dynamics. Their presented strategy relies principally on the use of the spherical coordinate method where the desired position of the follower quadrotor is specified using a desired separation distance along with a desired angle of incidence and bearing. The model unknown nonlinearities are compensated using the neural network techniques. However, a common drawback of many previous leader-follower formation controllers is that they ignore the physical quadrotor flight limitation. In fact, for a safe flight, it is required that the quadrotor avoid singularities in the rotation matrix represented by the Euler angles. Essentially, they often assume that the quadrotor system is always away from the singularity points and that the quadrotor does not rotate too much. From a practical viewpoint, the trajectory generated by the leader vehicle might be aggressive sometimes. Consequently, the follower quadrotor is most likely exposed to a fall in singularity points. This, in turn, may result in poor tracking performance of the proposed controller. An immediate solution to alleviate this problem is to constrain the variation of the quadrotor states within a specified range, then design a controller such that the quadrotor's state never transgresses these constraints.

1.2. Contributions and Novelties. Motivated by the earlier works, the main purpose of this work is to tackle the distance-based formation control problem for a group of homogeneous quadrotor vehicles modeled by an undirected graph. Contrary to the current state of the art, limited explicit communication among neighboring quadrotors is mainly motivated to avoid flooding the communication bandwidth in real-time applications, particularly when the number of cooperating quadrotors increases. To keep communication to a minimum, we propose a new distance-based formation control protocol for a group of multiple quadrotors in a leader-follower architecture, where sensor constraints are explicitly addressed in the design. In this architecture, we assume that the target's relative position with a leader in the group can be shared among other follower quadrotors, while its velocity is made unavailable. To learn this reference velocity, an estimation mechanism is implemented on each quadrotor so that a predefined formation is recovered so the quadrotors maintain a desired distance among their neighboring followers, while avoiding collision and ensuring relative localization. To deal with underactuation of the quadrotor vehicle in the formation, a decentralized intermediary translational control input is designed for relative position tracking, by which a bounded control thrust and bounded desired orientation are extracted. Then, a control torque for each individual quadrotor is designed to track the desired orientation while avoiding overturn of the quadrotors.

In comparison with existing works, the main contributions of this paper are listed as follows:

(1) Compared to [6, 26, 27], our controller is completely designed independently from a global reference coordinate and does not require the local frame of all vehicles to be aligned. Only the distance requirements are used with local sensors to ensure formation maintenance

(2) Our controller is decentralized and ensures simultaneously collision avoidance and self-localization. As opposed to [6, 28], the control input for the translational dynamics is not designed based on a negative gradient of specific local/global potential functions; it is designed using a barrier Lyapunov function ensuring convergence to the appropriate distances with predefined performances

(3) The output constraints on the orientation angles are handled using the integral barrier Lyapunov (iBL) function [29] in the control design, thus relaxing the assumption on small orientation angles in [30–32] and therefore ensuring that the quadrotor will never overturn

(4) Our design is modular in the sense that the stability of the cooperative system is easily shown by the fact that the closed-loop system is regarded as cascaded systems in which the position dynamic subsystem is the driven subsystem while the orientation subsystem is the driving subsystem

1.3. Organization. The paper is organized as follows. The upcoming section introduces basic concepts of rigid graph theory and results on the stability of cascade systems. Section 3 models the dynamic equations of motion for an individual quadrotor and presents the decentralized distance-based formation control objectives. The controllers for the translational and rotational dynamics of the quadrotors in the group formation are introduced in Section 4. The main result and the convergence analysis for the proposed controller are provided in Section 5. Numerical simulations are presented in Section 6. Finally, the conclusion is presented in Section 7.

2. Preliminaries

In this section, we present concepts of rigid graph theory for the control formulation taken from [33] and a lemma from [34] for the stability analysis of nonautonomous nonlinear systems, in cascade, which will be useful to establish the stability of the whole closed-loop system.

An undirect graph $\mathcal{G}$ with pair (v, ε) is defined as a set of vertices $V = 1, \cdots, n$ connected with a set of undirected edges $\mathcal{E}$ such that if the edge (i, j) in $\mathcal{E}$,then $(j, i) \in \varepsilon$. The number of edges that amounts for the connection between the vertices is $l = 1, \cdots, n(n-1)/2$. The set of neighbors of vertex i is defined as $\mathcal{N}(\varepsilon)$ such that $\mathcal{N}(\varepsilon) = \{j \in v | (i, j)| \in \varepsilon\}$. A framework of $\mathcal{G}$ is the pair $\mathcal{F} = (\mathcal{G}, \bar{\mathbf{p}})$, where $\bar{\mathbf{p}} \in \mathbb{R}^{3n}$ is the stack vector containing the position of all quadrotors. The rigidity function associated with $\mathcal{F}$ is denoted by $\Lambda(\bar{\mathbf{p}})$ and is given by $\Lambda(\bar{\mathbf{p}}) = [\cdots, \|\mathbf{p}_i - \mathbf{p}_j\|_2^2, \cdots]^\top$, $(i, j) \in \varepsilon$, where $\|\bullet\|_2^2$ denotes the Euclidian norm. The rigidity matrix $M : \mathbb{R}^{3n} \longrightarrow \mathbb{R}^{l \times 3n}$ of $\mathcal{F} = (\mathcal{G}, \bar{p})$ is defined as $M = (1/2)(\partial\Lambda(\bar{\mathbf{p}})/\partial(\bar{\mathbf{p}}))$. It can be shown similarly to [35] that rank $(M) = 3n - 6$. It follows that $\mathcal{F}$ is infinitesimally rigid [33] in $\mathbb{R}^3$ if the corresponding graph has at least $3n - 6$ edges. An isometry of $\mathbb{R}^3$ is a bijective map $\mathcal{J} : \mathbb{R}^3 \longrightarrow \mathbb{R}^3$ satisfying $\|v - \varpi\| = \|\mathcal{J}(v) - \mathcal{J}(\varpi)\|$, $v, \varpi \in \mathbb{R}^3$. Two frameworks are said to be isomorphic in $\mathbb{R}^3$ if they are related by isometry. The set of all frameworks that is isomorphic to $\mathcal{F}$ is denoted by Iso$(\mathcal{F})$. Frameworks $(\mathcal{G}\bar{\mathbf{p}})$ and $(\mathcal{G}\hat{\bar{\mathbf{p}}})$ are equivalent if $\Lambda(\bar{\mathbf{p}}) = \lambda(\hat{\bar{\mathbf{p}}})$ and are congruent if $\|\mathbf{p}_i - \mathbf{p}_j\| = \|\hat{\mathbf{p}}_i - \hat{\mathbf{p}}_j\|, \forall i, j \in \mathcal{V}$. If the infinitesimally rigid frameworks $(\mathcal{G}\bar{\mathbf{p}})$ and $(\mathcal{G}\hat{\bar{\mathbf{p}}})$ are equivalent but not congruent, they are called ambiguous. The collection of frameworks which are ambiguous to the infinitesimally rigid frameworks is denoted by Amb$(\mathcal{F})$.

Lemma 1 (see [33]). *Given a vector $\mathbf{x} \in \mathbb{R}^3$ and let 1_n be the $n \times 1$ vector of ones, then $M(\bar{\mathbf{p}})(1_n \otimes \mathbf{x}) = 0$.*

Lemma 2. (see [33]). *If the framework $\mathcal{F} = (\mathcal{G}, \bar{\mathbf{p}})$ is minimally and infinitesimally rigid, the the matrix $M(\bar{\mathbf{p}})M(\bar{\mathbf{p}})^\top$ is positive definite.*

Definition 3. A continuous function $\alpha : [0, a) \longrightarrow [0,\infty)$ is said to belong to class $\mathcal{K}$ if it is strictly increasing and $\alpha(0) = 0$. It is said to belong to class $\mathcal{K}_\infty$ if $a = \infty$ and $\lim_{r\to\infty}\alpha(r) = \infty$. A continuous function $\beta(.,.)$: $[0, a) \times [0, a) \longrightarrow [0,\infty)$ is said to belong to class $\mathcal{KL}$ if, for each fixed s, the mapping $\beta(r, s)$ belongs to class $\mathcal{K}$ with respect to r and, for each fixed r, the mapping $\beta(r, s)$ is decreasing with respect to s and $\beta(r, s) \longrightarrow 0$ as $s \longrightarrow \infty$.

Lemma 4. (see [34]). *Consider the following cascade system:*

$$\begin{aligned} \dot{\mathbf{x}} &= f(\mathbf{x}) + \Phi(\mathbf{x}, z), \\ \dot{\mathbf{z}} &= G(\mathbf{z}). \end{aligned} \tag{1}$$

If the equilibrium $\mathbf{x} = 0$ is GAS/LES and the equilibrium $\mathbf{z} = 0$ is LES and assume also that there exists a constant $\ell_1 \geq 0$ and a C_1-$\mathcal{K}$ function $\gamma(.)$, differentiable at $\mathbf{z} = 0$ where

$$\|\Phi(\mathbf{x}, \mathbf{y})\| \leq \gamma(\mathbf{z})\|\mathbf{x}\|. \tag{2}$$

If in addition there exists a positive semidefinite radially unlimited function $W(\mathbf{x})$ and some positive constants ℓ_2 and ℓ_3 such that $\|\mathbf{x}\| \geq \ell_2$

$$\begin{aligned} &\frac{\partial W}{\partial \mathbf{x}} f(\mathbf{x}) \leq 0, \\ &\left\|\frac{\partial W}{\partial \mathbf{x}}\right\| \|\mathbf{x}\| \leq \ell_3 W(\mathbf{x}), \end{aligned} \tag{3}$$

then the equilibrium point $(\mathbf{x}, \mathbf{y}) = (0, 0)$ is LES.

3. Problem Formulation

The proposed formation scheme is to coordinate the motion of n quadrotors under the leader-follower architecture. The leader quadrotor in the group is indexed by n, while the rest of the follower vehicles update their state with locally available information. The formation control scheme to be addressed in this paper will be formulated as formation maneuvering and target interception problems as in [33]. Hereafter, the interaction among the vehicles is modeled by undirected graphs $\mathcal{G} \coloneqq (\mathcal{V}, \mathcal{E})$ where $\mathcal{V} = \{1, \cdots, i, \cdots, n\}$ is the set of vertices (quadrotors) and $\mathcal{E} \subset \mathcal{V} \times \mathcal{V}$ is the set of edges representing the connectivity among the vehicles. Define the set of neighbors of the i-th quadrotor as $\mathcal{N}_i = \{j \in \mathcal{V} | (i, j) \in \mathcal{E}\}$.

3.1. Quadrotor Model Dynamics. To develop the quadrotor's equations of motion, we first defined two reference frames. The first one is the earth-fixed inertial frame defined as $I = \{O_I, x_I, y_I, z_I\}$, and the second is a body-fixed frame denoted by $\mathbf{B} = \{O, x_b, y_b, z_b\}$ whose origin O is located at the quadrotor's center of gravity (CG) as shown in Figure 1.

Let $\mathbf{p}_i \in \mathbb{R}^3$ be the three-dimensional position of the i-th quadrotor and the rotation matrix $\mathbf{R}_i \in \mathrm{SO}(3)$ parameterized with respect to the three Euler angles $\Theta_i = [\phi_i, \theta_i, \psi_i]^\top$ with ϕ_i, θ_i, and ψ_i being the roll, pitch, and yaw angles, respectively, and where the special Euclidean group $\mathrm{SO}(3)$ is the group of 3×3 orthogonal matrices with a determinant of one, i.e., $\mathrm{SO}(3) = \{\mathbf{R}_i \in \mathbb{R}^{3\times 3} | \mathbf{R}_i^\top \mathbf{R}_i = I, \det(\mathbf{R}_i) = 1\}$. Following the standard results, the associated orientation dynamics are governed by

$$\dot{\Theta}_i = \Psi_i(\Theta)\Omega_i, \tag{4}$$

where

$$\Psi_i(\Theta_i) = \begin{bmatrix} 1 & \sin\phi_i \tan\theta_i & \cos\phi_i \tan\theta_i \\ 0 & \cos\phi_i & -\sin\phi_i \\ 0 & \dfrac{\sin\phi_i}{\cos\theta_i} & \dfrac{\cos\phi_i}{\cos\theta_i} \end{bmatrix}. \tag{5}$$

The kinematic and dynamic equations of motion of the i-th quadrotor are given by

$$\dot{\mathbf{p}}_i = v_i, \tag{6}$$

$$m_i \dot{v}_i = m_i g e_z - f_i \mathbf{R}_i e_z + \Delta_{xi}, \tag{7}$$

$$\dot{\mathbf{R}}_i = \mathbf{R}_i \mathbf{S}(\Omega_i), \tag{8}$$

$$J_i \dot{\Omega}_i = -\Omega_i \times J_i \Omega_i + \tau_i + \Delta_{\Omega i}, \tag{9}$$

where $v_i = [v_{xi}, v_{yi}, v_{zi}]^\top \in \mathbb{R}^3$ is the linear velocity vector in inertial coordinates, $\Omega_i = [\omega_{xi}, \omega_{yi}, \omega_{zi}]^\top \in \mathbb{R}^3$, $m \in \mathbb{R}$ denotes the total mass of the quadrotor i, $J_i \in \mathbb{R}^3$ is the inertia matrix with respect to the frame $\mathbf{B}$, $e_z = (0, 0, 1)^\top$ is the unit vector, and g is the gravitational acceleration. The thrust magnitude is denoted as $f_i \in \mathbb{R}$, and $\tau_i \in \mathbb{R}^3$ is the moment vector; both are considered as the control inputs of the quadrotor. The matrix $\mathbf{S}(\Omega_i)$ is a skew-symmetric matrix containing the elements of the body-fixed angular velocity Ω_i. Denote by Δ_{xi} and $\Delta_{\Omega i}$ the unstructured uncertainties in the translational dynamics and the rotational dynamics of a quadrotor, respectively. We further assume that the uncertainties Δ_{xi} and $\Delta_{\Omega i}$ are small time varying and bounded, that is,

$$\|\Delta_{xi}\| \le \delta_{xi}, \ \|\Delta_{\Omega i}\| \le \delta_{\Omega i}, \tag{10}$$

where δ_{xi} and $\delta_{\omega i}$ are known constants. From the dynamic equations (7)–(9), it is worth noting that the quadrotor is an underactuated system with only one degree of freedom for the thrust actuation in the body frame, while the attitude dynamics are fully actuated and can be used to drive the thrust force to any desired orientation.

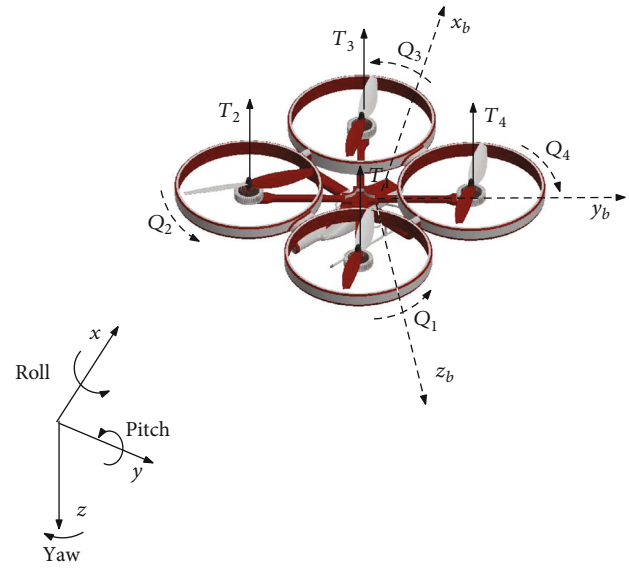

Figure 1: Rigid quadrotor UAV configuration.

3.2. Control Objective. The leader-follower approach considered in this paper assumes a group of n quadrotor vehicles with the n-th vehicle set to be the leader which can merely measure the target's relative position $\mathbf{p}_d(t) \in \mathbb{R}^3$. Additionally, it is also assumed that the only information that the quadrotors can sense is exclusively acquired from their local sensors. The control objective is to design controllers for the group of vehicles to maintain interdistance specification $d_{ij}^\star \in \varepsilon$ among the vehicles to attain a rigid desired formation, while guaranteeing formation maintenance and inter-vehicle collision, that is, if the desired formation is modeled by the framework $F^* = (\mathcal{G}^*, \mathbf{p}^*)$, which is assumed to be infinitesimally and minimally rigid, where $F^* = (v^*, \mathcal{E}^*)$ and $\mathbf{p}^* = [\mathbf{p}_1^{*\top}, \mathbf{p}_2^{*\top}, \cdots, \mathbf{p}_n^{*\top}]^\top$ are the collection of the targets' positions. Also, considering that the actual formation of quadrotors is modeled by $F(t) = (\mathcal{G}^*, \bar{\mathbf{p}})$, then the formation control problem boils down to ensure the following:

$$F(t) \longrightarrow \mathrm{Iso}(F^*), \quad \text{as } t \longrightarrow \infty. \tag{11}$$

Mathematically speaking, the control objective reduces to design a desired thrust magnitude for the system dynamics of each quadrotor vehicle (7) such that

$$\begin{aligned} &\lim_{t\to\infty} \left\|\mathbf{p}_i - \mathbf{p}_j\right\| - d_{ij}^\star = 0, \\ &\lim_{t\to\infty} (v_i(t) - v_d(t)) = \epsilon, \\ &\forall (i, j) \in \varepsilon, \end{aligned} \tag{12}$$

where $v_d(t) \in \mathbb{R}^3$ is a bounded, continuous function designating the translational velocity of the formation and is a positive limit upper-bound. An important issue in the

formation of multiple quadrotor vehicles is to ensure safe navigation by avoiding collision among interacting vehicles. To this end, the distance that separates the quadrotors should be kept greater than a safety zone. Similarly, the quadrotors should also be retained within the connectivity network to achieve the group tasks. The decentralized controller should also satisfy the following constraint:

$$-\underline{\rho}_{ij}(t) < e_{ij}(t) < \bar{\rho}_{ij}(t) \quad \forall (i,j) \in \varepsilon, \tag{13}$$

where $e_{ij}(t) = \|\mathbf{p}_i - \mathbf{p}_j\| - d_{ij}^{\star}$ and $\bar{\rho}_{ij}(t) > 0, \underline{\rho}_{ij}(t) > 0$ are prescribed functions.In addition to the translational motion of the quadrotor, an essential part of the control is the attitude innermost layer of the controller. While the position controller calculates the desired direction of the thrust vector, the attitude controller will ensure the alignment of the real thrust vector with the desired one. A second control objective is to ensure a fast control loop for the attitude innermost layer. Thus, our goal is to satisfy the following limit:

$$\lim_{t\to\infty} \mathbf{R}_i(t) = \mathbf{R}_{di}(t), \quad \forall t > 0, \tag{14}$$

where $\mathbf{R}_{di}(t)$ represents the desired attitude that is calculated based on the desired trust vector f_{di} which will be derived later in the next section.

4. Control Design

4.1. Decentralized Control Design for the Position Outer-Loop. In this section, we will use the backstepping technique to derive a decentralized cooperative controller for the position control loop in the sense that each quadrotor requires the relative position of its neighbors and its own velocity, while ensuring collision avoidance among the vehicles. For that purpose, the vector term $f_i \mathbf{R}_i e_z$ will be considered as the control input signal for the cooperative position-tracking task. It is common to assign to that input signal a desired value $f_{di}\mathbf{R}_{di}e_z$ that we wish to reach in the final stabilization process. $\mathbf{R}_{di}$ denotes the desired orientation of the follower quadrotor while $\mathbf{R}_{di}e_z$ represents the direction of the force amplitude f_{di}

Assumption 5. The actuator dynamics of the follower quadrotor are negligible with respect to the rigid body dynamics of the quadrotor.

Due to the dynamics consideration, Assumption 5 reveals that the desired thrust magnitude f_{di} can be instantaneously reached by the force control input f_i; therefore, it is straightforward to conclude that $f_{di}\mathbf{R}_{di}e_z = f_i\mathbf{R}_{di}e_z$. Hence, the first two equations in (7) can be rewritten in terms of $\mathbf{R}_{di}$ and $\mathbf{R}_i$ as follows:

$$\dot{\mathbf{p}}_i = v_i, \tag{15}$$

$$m_i\dot{v}_i = m_i g e_z - f_i\mathbf{R}_{di}e_z + \tilde{\mathbf{h}}_i(f_i, \mathbf{R}_i, \mathbf{R}_{di}) + \Delta_{xi}, \tag{16}$$

where the coupling term $\tilde{\mathbf{h}}_i(f_i, \mathbf{R}_i, \mathbf{R}_{di}) = -f_i(\mathbf{R}_i - \mathbf{R}_{di})e_z$ which can be written as $\tilde{\mathbf{h}}_i(f_i, \mathbf{R}_i, \mathbf{R}_{di}) = -f_i(\widetilde{\mathbf{R}_i} - I)\mathbf{R}_{di}e_z$, where $\tilde{\mathbf{R}}_i = \mathbf{R}_i\mathbf{R}_{di}^{\top}$ is the rotation matrix error. Thus, system (15) can be viewed as a nominal system, perturbed by a bounded term of the orientation error, which is assumed to converge to zero faster than the closed-loop translational dynamics by ensuring that $\tilde{\mathbf{R}}_i = I$ or, in other words, by designing an attitude control law that ensures that $\mathbf{R}_i$ converges to $\mathbf{R}_{di}$ as time goes to infinity. For this reason and to design the position control law, we will make the following assumption.

Assumption 6. Since the closed-loop attitude dynamics is faster than the translational dynamics, then it is logical to consider that $\mathbf{R}_i = \mathbf{R}_{di}$.

Remark 7. It is important to mention that Assumption 6 is only useful to help for the design of the control law position without explicitly accounting for the orientation tracking error $\tilde{\mathbf{R}}_i$ in the translational dynamics. The stability analysis of the resulting translational error dynamics with the coupling term will be investigated in detail later on in Section 5.

To help for the development of the decentralized cooperative controller, we first define the following state variable:

$$\ell_{ij} = \left\|\tilde{\mathbf{p}}_{ij}\right\|^2 - d_{ij}^{\star 2}, \tag{17}$$

where $\|\tilde{\mathbf{p}}_{ij}\| = \|\mathbf{p}_i - \mathbf{p}_j\|$ from the definition of the relative distance, it can be easily seen that $\ell_{ij} = e_{ij}(e_{ij} + 2d_{ij}^{\star})$ which can be shown to be constrained as

$$\underline{\ell}_{ij}\ell(t)^{\star} < \ell_{ij} < \bar{\ell}_{ij}\ell^{\star}(t), \tag{18}$$

where $\ell^{\star}(t) = 2\ell(t)$ is a performance function chosen similar to [36], such that it enforces transient and steady state performance specifications on the state variable ℓ_{ij}. As such, $\ell(t) = (\ell_0 - \ell_\infty)e^{-at} + \ell_\infty$, where $\ell_0, \ell_\infty > 0$ are performance specifications and $a > 0$. Owing to the decreasing property of the performance function, one can see that $-\underline{\ell}_{ij}\ell_0$ and $\bar{\ell}_{ij}\ell_0$ serve as the maximum allowed overshoot and the minimum allowed undershot of ℓ_{ij}, respectively. The control design proceeds as follows:

Step 1. It is important to transform the control problem with the constraint (18) into an unconstrained one. To this end, the following barrier function is defined; it is a subtle treatment for ensuring collision avoidance and connectivity maintenance [37]:

$$z_{ij} = T\left(\frac{\ell_{ij}}{2\ell}\right) = \ln\left(\underline{\ell}_{ij}\bar{\ell}_{ij} - \frac{\bar{\ell}_{ij}\ell_{ij}}{2\ell}\right) - \ln\left(\underline{\ell}_{ij}\bar{\ell}_{ij} - \frac{\underline{\ell}_{ij}\ell_{ij}}{2\ell}\right). \tag{19}$$

Clearly, from definition (19), if the variable z_{ij} is bounded, then ℓ_{ij}/ℓ remains within the interval $(-\underline{\ell}_{ij}, \bar{\ell}_{ij})$ for all $t \geq 0$; therefore, the constraints in (18) are satisfied. Furthermore, it is straightforward to show that $T^{-1}(z_{ij}) = \underline{\ell}_{ij}\bar{\ell}_{ij}(e^{z_{ij}} - 1)/(\underline{\ell}_{ij}e^{z_{ij}} - \bar{\ell}_{ij})$, then when $z_{ij} = 0$, we have $\ell_{ij} = 0$.

The time derivative of the state variable of z_{ij} considering (17) and (19) is

$$\dot{z}_{ij} = \frac{1}{2}\eta_{ij}\left(\dot{\ell}_{ij} - \varpi_j\right) = \eta_{ij}\left(\tilde{\mathbf{p}}_{ij}^{\top}\left(v_i - v_j\right) - \varpi_{ij}\right), \tag{20}$$

where

$$\eta_{ij} = \frac{\partial T(.)}{\partial\left(\ell_{ij}/\ell\right)}\frac{1}{\ell},\ \varpi_{ij} = \frac{\dot{\ell}}{\ell}\ell_{ij}. \tag{21}$$

For the dynamic system (20), design the following velocity profile:

$$\vartheta_{di} = -k\sum_{j\in\mathcal{N}(\varepsilon)}\eta_{ij}\tilde{\mathbf{p}}_{ij}^{\top}z_{ij} + \frac{1}{\lambda_{\min}(MM^{\top})}\sum_{j\in\mathcal{N}(\varepsilon)}\eta_{ij}\tilde{\mathbf{p}}_{ij}^{\top}\varpi_{ij} + \hat{v}_d, \tag{22}$$

where $k > 0$ is a design parameter, $\lambda_{\min}(.)$ denotes the minimum eigenvalue, and $\hat{v}_d$ is the estimate of the target velocity in which position is only available to the leader vehicle. The estimate of the target velocity is the output of the following filter designed in a similar way as in [38]:

$$\begin{aligned}\hat{v}_d &= -\hbar_{1i}(\varphi_i) - \hbar_{2i}(\varphi_i),\\ r_{ei} &= \varphi_i + \rho_e,\ \varphi_i(0) = 0,\\ \dot{\varphi}_i &= -\hbar_{1i}(\varphi_i)\mathbf{K}r_{ei},\end{aligned} \tag{23}$$

where $\hbar_{1i}(\varphi_i) = [c_1\tanh(\varphi_{1i}/c_1), c_2\tanh(\varphi_{2i}/c_2), c_3\tanh(\varphi_{3i}/c_3)]^{\top}$ and $\hbar_{2i}(\varphi_i) = [k_1\tanh(\varphi_{1i}/k_1), k_2\tanh(\varphi_{2i}/c_2), k_3\tanh(\varphi_{3i}/c_3)]^{\top}$, and $c_m, k_m > 0$, $m = 1, 2, 3$ are design parameters, $\mathbf{K} = \mathrm{diag}(k_1, k_2, k_3)$, and $\rho_e = \mathbf{p}_n(t) - \hat{\mathbf{p}}_d(t)$ is the interception error between the leader quadrotor and the target, with $\hat{\mathbf{p}}_d(t) = \hat{v}_d(t)$.

Step 2. In this step, define the velocity tracking error as

$$v_{ei} = v_i - \vartheta_{di}. \tag{24}$$

Taking the time derivative of (24) along the solutions of the second equation of (15) results in

$$m_i\dot{v}_{ei} = m_i g e_z - f_i\mathbf{R}_{di}e_z + \Delta_{xi} - m_i\dot{\vartheta}_{di}. \tag{25}$$

Note that the term $\tilde{\mathbf{h}}_i(f_i, \mathbf{R}_i, \mathbf{R}_{di})$ is temporarily ignored at this stage of the design. It will, however, be investigated in a later stage of the stability analysis. It becomes easy from (25) to select the thrust force f_i that stabilizes v_{ei} to the origin. It is also important to point out that the total thrust force to be designed must be limited such that actuators' physical limitations are not violated. By defining the saturated input $U_i = f_i\mathbf{R}_{di}e_z$ and the nominal input as $U_{0i} = f_{0i}\mathbf{R}_{di}e_z$, then this unsaturated input is designed as

$$U_{0i} = k_{2i}v_{ei} + m_i g e_z - m_i\dot{\vartheta}_{di} + \hat{\Delta}_{xi} + k_{1i}\xi_i, \tag{26}$$

where k_{1i} and k_{2i} are design parameters and ξ_i is an auxiliary state system generated as

$$\dot{\xi}_i = \begin{cases} -K_{\xi i}\xi_i - g_i\xi_i + \varsigma_i\Delta U_i, & \text{if } |\xi_{mi}| > v_i,\ m = 1, \cdots, 3,\\ 0, & \text{if } |\xi_{mi}| > v_i,\ m = 1, \cdots, 3,\end{cases} \tag{27}$$

where $\xi = [\xi_{1i}, \xi_{2i}, \xi_{3i}]^{\top}$, $v_i > 0$, is a small number; $K_{\xi i} > 1$, $\varsigma_i > 0$, are design constants; $\Delta U_i = U_i - U_{0i}$, and $g_i = |v_{ei}^{\top}\Delta U_i + 0.5\varsigma_i^2\Delta U_i^{\top}\Delta U_i|/\|\boldsymbol{\xi}_i\|^2$. More discussion about the auxiliary system to overcome the saturation effect of the control input can be found in [39]. $\hat{\Delta}_{xi}$ is the estimate of the disturbance Δ_{xi}, generated using the following disturbance observer [40]:

$$\hat{\Delta}_{xi} = \varrho_{xi} + K_{xi}m_i v_{ei}, \tag{28}$$

$$\dot{\varrho}_{xi} = K_{xi}\varrho_{xi} - K_{xi}\left(m_i g e_z - f_i\mathbf{R}_{di}e_z - m_i\dot{\vartheta}_{di} + K_{xi}m_i v_{ei}\right), \tag{29}$$

where K_{xi} is s a symmetric and positive definite matrix.

The following proposition summarizes the distributed cooperative control for the translational dynamics of the set of quadrotors in the formation.

Proposition 8. *Consider the formation of a group of quadrotors, given the translational dynamics for each quadrotor in group (15), under Assumptions 5 and 6, if the nominal thrust magnitude f_{0i} and its direction $\mathbf{R}_{di}e_z$ are selected according to (30) and (31)*

$$f_{0i} = \left\|k_{2i}v_{ei} + m_i g e_z - m_i\dot{\vartheta}_{di}\left(\hat{\dot{v}}_d\right) + \hat{\Delta}_{xi} + k_{1i}\xi_i\right\|, \tag{30}$$

$$\mathbf{R}_{di}e_z\frac{k_{2i}v_{ei} + m_i g e_z - m_i\dot{\vartheta}_{di}\left(\hat{\dot{v}}_d\right) + \hat{\Delta}_{xi} + k_{1i}\xi_i}{\left\|k_{2i}v_{ei} + m_i g e_z - m_i\dot{\vartheta}_{di}\left(\hat{\dot{v}}_d\right) + \hat{\Delta}_{xi} + k_{1i}\xi_i\right\|}, \tag{31}$$

where $\hat{v}_d = [v\wedge_{xd}, v\wedge_{yd}, v\wedge_{zd}]^{\top} \in \mathbb{R}^3$ is the estimate of the target velocity using filter (23), then the equilibrium $(z_{ij}, v_{ei}^{\top}, \xi_i^{\top})^{\top} = 0$ of the closed-loop system is globally asymptotically stable (GAS). Furthermore, the velocity vector of the leader quadrotor uniformly semiglobally practical asymptotically converges to $v_d(t)$.

Proof. The proof proceeds in two folds: In a first stage, we show that the desired formation is attained with prescribed transient performance, while avoiding interagent collision and connectivity intermittent by ensuring that the leader vehicle tracks an estimate of the target's state quite accurately. In a second stage, we show that the estimate of the target's velocity

converges to a vicinity of its true value. To proceed, we first define the following candidate Lyapunov function:

$$V_1 = \frac{1}{2} z^\top z, \tag{32}$$

where $z = [\cdots, z_{ij}, \cdots]^\top \in \mathbb{R}^p$, $(i,j) \in \varepsilon$. Differentiating V_1 along the solutions of (20) results in

$$\dot{V}_1 = z^\top \Upsilon M \bar{v} - z^\top \Upsilon \Gamma, \tag{33}$$

where $\Upsilon = \text{diag}\,(\eta_{ij}) \in \mathbb{R}^{p\times p}$, $\Gamma = [\varpi_{1j}, \varpi_{2j}, \cdots, \varpi_{nj}]^\top \in \mathbb{R}^l$, and $\bar{v} = [v_1^\top, v_2^\top, \cdots, v_n^\top]^\top \in \mathbb{R}^{3n}$. Let $\bar{\vartheta}_d = [\vartheta_{d1}^\top, \vartheta_{d2}^\top, \cdots, \vartheta_{dn}^\top]^\top \in \mathbb{R}^{3n}$, then adding and subtracting the term $z^\top \Upsilon M \bar{\vartheta}_d$ and substituting the expression ϑ_{di}, $i = 1, \cdots, n$, from the velocity protocol (22), using Lemmas 1 and 2, we obtain

$$\begin{aligned}
\dot{V}_1 &= -kz^\top \Upsilon M M^\top \Upsilon + z \Upsilon M \bar{v}_e \\
&\quad - \frac{MM^\top}{\lambda_{\min}(MM^\top)} z^\top \Upsilon \Gamma + z^\top \Upsilon \Gamma + z^\top \Upsilon M (1_n \otimes \hat{v}_d) \\
&\le -kz^\top \Upsilon M M^\top \Upsilon + z^\top \Upsilon M \bar{v}_e \\
&\le -\left(kb_0 - \frac{1}{2_j} \right) z^\top z + \frac{j}{2} b_0 \bar{v}_e^\top \bar{v}_e,
\end{aligned} \tag{34}$$

where $b_0 = \lambda_{\min}(\Upsilon M M^\top \Upsilon)$ and j is a parameter chosen such that $k > 1/2b_0 j$. Note that the second term on the right-hand side of inequality (34) will be dealt with in a further step of the backstepping procedure. In the sequel, let us consider the following positive definite Lyapunov function:

$$V_2 = V_1 + \frac{1}{2} \sum_{i=1}^n m_i v_{ei}^\top v_{ei} + \frac{1}{2} \sum_{i=1}^n \tilde{\Delta}_{xi}^\top \tilde{\Delta}_{xi} + \frac{1}{2} \sum_{i=1}^n \xi_i^\top \xi_i, \tag{35}$$

where $\tilde{\Delta}_{xi} = \Delta_{xi} - \widehat{\Delta}_{xi}$ represents the estimation error of the disturbances affecting the transitional dynamics of the follower quadrotor. Take the time derivative of (35) along the solutions of (25), (27), (28), and (34) and substituting the control (30) and (31) we obtain

$$\begin{aligned}
\dot{V}_2(t) &= \dot{V}_1 + \sum_{i=1}^n m_i v_{ei}^\top \dot{v}_{ei} + \sum_{i=1}^n \tilde{\Delta}_{xi}^\top \dot{\tilde{\Delta}}_{xi} + \sum_{i=1}^n \xi_i^\top \dot{\xi}_i \\
&\le -\left(kb_0 - \frac{1}{2j} \right) z^\top z + \frac{j}{1} b_0 \sum_{i=1}^n v_{ei}^\top v_{ei} \\
&\quad + \sum_{i=1}^n v_{ei}^\top \left(m_i g e_z - U_{io} - \Delta U_i + \Delta_{xi} - m_i \dot{\vartheta}_{di} \right) \\
&\quad + \sum_{i=1}^n \tilde{\Delta}_{xi}^\top \dot{\tilde{\Delta}}_{xi} + \sum_{i=1}^n \xi_i^\top \dot{\xi}_i \\
&\le -\left(kb_0 - \frac{1}{2j} \right) z^\top z - \sum_{i=1}^n \left(k_{2i} - \frac{j}{2} b_0 \right) v_{ei}^\top v_{ei} \\
&\quad - \sum_{i=1}^n K_{xi} \tilde{\Delta}_{xi}^\top \tilde{\Delta}_{xi} - \sum_{i=1}^n K_\xi \xi_i^\top \xi_i \le -a_z V_2(t),
\end{aligned} \tag{36}$$

where $a_z = 2 \min \{(kb_0 - 1/2j), (k_{2i} - (j/2)b_0), K_{xi}, K_\xi\}$. From (36), it is clear that $\dot{V}_2 \le 0$; therefore, $V_2(t)$ is decreasing for all $t \ge 0$ from which it can be concluded that z, v_{ei}, Δ_{xi}, and ξ_i are all bounded. Thus, there exists a positive constant $\bar{z}$ such that $z \in \Psi_z \triangleq, \{z \in \mathbb{R}^p : \|z\| \le \bar{z}\}, \forall t \ge 0$, which from (19), by noting that $\ell_{ij}/2\ell = T^{-1}(z_{ij}) = \bar{\ell}_{ij}\underline{\ell}_{ij}(e^{z_{ij}} - 1)/(\underline{\ell}_{ij} e^{z_{ij}} - \bar{\ell}_{ij})$, we have $-\underline{\ell}_{ij} < \bar{\ell}_{ij}\underline{\ell}_{ij}(e^{-\bar{z}} - 1)/(\underline{\ell}_{ij} e^{-\bar{z}} - \bar{\ell}_{ij}) \le \ell_{ij}/2\ell \le \bar{\ell}_{ij}\underline{\ell}_{ij}(e^{\bar{z}} - 1)/(\underline{\ell}_{ij} e^{\bar{z}} - \bar{\ell}_{ij})$. That is, $\ell_{ij}/2\ell$ remains within the compact set $[\bar{\ell}_{ij}\underline{\ell}_{ij}(e^{-\bar{z}} - 1)/(\underline{\ell}_{ij} e^{-\bar{z}} - \bar{\ell}_{ij}) \le \ell_{ij}/2\ell, \bar{\ell}_{ij}\underline{\ell}_{ij}(e^{\bar{z}} - 1)/(\underline{\ell}_{ij} e^{\bar{z}} - \bar{\ell}_{ij})]$ of $(\underline{\ell}_{ij}, \bar{\ell}_{ij})$, from which it is straightforward to conclude that relative distance performance among the quadrotors in group (18) is guaranteed. Additionally, from (36), the equilibrium point $(z^\top, v_{ei}^\top, \tilde{\Delta}^\top{}_{xi}, \xi_i^\top) = 0^\top$ is exponentially stable for all $t \ge 0$.

Thus, it can be concluded that $\lim_{t\to\infty} \ell_{ij} = 0, \forall (i,j) \in \mathscr{E}$. Also, from (22), it can be deduced that $\lim_{t\to\infty} \vartheta_{di}(t) = \hat{v}_d$.

The second stage of the proof is to show that the estimate of the leader's velocity converges to a neighborhood of the target's true velocity. In this direction, following [38], a Lyapunov function candidate is proposed as $V_3 = (1/2)\sum_{i=1}^n r_{ei}^\top r_{ei} + \sum_{i=1}^n \nu_i(\varphi_i)^\top \nu_i(\varphi_i)$, where $\nu(\varphi_i) = [\sqrt{k_i \log(\cosh(\varphi 1_i/k_i)}, \sqrt{k_2 \log(\cosh(\varphi 2_i/k_2)}, \sqrt{k_3 \log(\cosh(\varphi 3_i/k_3)}]^\top$. The time derivative of V_3 along the solutions of filter (23) yields

$$\begin{aligned}
\dot{V}_3 &= \sum_{i=1}^n r_{ei}^\top \dot{r}_{ei} + \mathbf{K}^{-1} \sum_{i=1}^n \dot{\varphi}_i^\top \bar{h}_{2i}(\varphi_i) \\
&= \sum_{i=1}^n r_{ei}^\top \left(-\mathbf{K} r_{ei} + \bar{h}_{2_i}(\varphi_i) + \hat{v}_n \right) + \mathbf{K}^{-1} \sum_{i=1}^n \dot{\varphi}_i^\top \bar{h}_{2i}(\varphi_i) \\
&= -\mathbf{K} \sum_{i=1}^n r_{ei}^\top r_{ei} - \mathbf{K}^{-1} \sum_{i=1}^n \bar{h}_{1i}(\varphi_i)^\top \bar{h}_{2i}(\varphi_i) + \sum_{i=1}^n r_{ei}^\top \hat{v}_n.
\end{aligned} \tag{37}$$

Since we showed that $v_{ei}, \forall i = 1, \cdots, n$, is bounded and so is ϑ_{di}, also by construction, $\hat{v}_d$ is bounded. It follows that there exists a constant V_n such that $\|v_n\| \le V_n$; therefore,

$$\begin{aligned}
\dot{V}_3 \le &-\left(\lambda \min(\mathbf{K}) - 0.5 - \frac{3V_n}{\|\bar{r}_e\|} \right) \sum_{i=1}^n \|r_{ei}\|^2 \\
&- \mathbf{K}^{-1} \sum_{i=1}^n \bar{h}_{1i}(\varphi_i)^\top \bar{h}_{2i}(\varphi_i),
\end{aligned} \tag{38}$$

where $\bar{r}_e = [r_{e1}, \cdots, r_{en}]^\top$. Letting b_0 be a given positive constant, we obtain for $\|r_{ei}\| \ge b_0$ the following bound for $\dot{V}_3$

$$\dot{V}_3 \le -\sum_{i=1}^n \|r_{ei}\|^2 - \mathbf{K}^{-1} \sum_{i=1}^n \bar{h}_{1i}(\varphi_i)^\top \bar{h}_{2i}(\varphi_i), \tag{39}$$

since $\bar{h}_{1i}(\varphi_i)^\top \bar{h}_{2i}(\varphi_i) \ge 0$; therefore, $\dot{V}_3 \le 0$; this shows that the solution of filter (23) is uniform semipractically asymptotically stable [23]. This completes the proof.

4.2. Control Design for the Attitude Inner-Loop. In this stage, the last two equations of (9) are considered. The moment vector τ_i will be designed to globally asymptotically and

locally exponentially stabilize the tracking error $\psi_i - \psi_{di}$ and the errors between the virtual controls of the roll and pitch angles and their actual values at the origin.

Step 1. Controlling the yaw angle.

The desired orientation $\mathbf{R}_{di}$ can be deduced from the expression of the rotation matrix $\mathbf{R}_i \in \mathrm{SO}(2)$ using its Euler angle parameterization subject to the constraint given by the specification of the desired yaw angle extracted from the translational system as shown in Figure 2. Indeed, in Figure 2, the angle $\tilde{\psi}_d$ represents the desired angle associated with the vector $\hat{v}_d(t)$ projected on the x-y plan. Clearly, when $v_i(t)$ matches with $\hat{v}_d(t)$, the yaw rate angle $\tilde{\psi}_i$ converges to zero. Following [41], the desired yaw angle is calculated by extracting yaw rate information from the cross- and inner-product of the desired velocity $\hat{v}_d(t)$ and the actual velocity $\boldsymbol{v}_i(t)$ as follows:

$$\begin{aligned}
\sin\left(\tilde{\psi}_i(t)\right) &= \frac{\hat{v}_d \times v_i}{\|\hat{v}_d\|\|v_i\|} = \frac{\sqrt{\left(v\wedge_{ydi}\dot{z}_i - v\wedge_{zdi}\dot{y}_i\right)^2 + \left(v\wedge_{zdi}\dot{y}_i - v\wedge_{ydi}\dot{z}_i\right)^2 + \left(v\wedge_{xdi}\dot{y}_i - v\wedge_{ydi}\dot{x}_i\right)^2}}{\sqrt{\left(\hat{v}_{xdi}^2 + \hat{v}_{ydi}^2 + \hat{v}_{zdi}^2\right)\left(\dot{x}_i^2 + \dot{y}_i^2 + \dot{z}_i^2\right)}},\\
\cos\left(\tilde{\psi}_i(t)\right) &= \frac{\hat{v}_d^{\top} v_i}{\|\hat{v}_d\|\|v_i\|} = \frac{\hat{v}_{xdi}\dot{x}_i + \hat{v}_{ydi}\dot{y}_i + \hat{v}_{zdi}\dot{z}_i}{\sqrt{\left(\hat{v}_{xdi}^2 + \hat{v}_{ydi}^2 + \hat{v}_{zdi}^2\right)\left(\dot{x}_i^2 + \dot{y}_i^2 + \dot{z}_i^2\right)}},\\
\tan\left(\tilde{\psi}_i(t)\right) &= \frac{\hat{v}_d \times v_i}{\hat{v}_d^{\top} v_i} = \frac{\sqrt{\left(v\wedge_{ydi}\dot{z}_i - v\wedge_{zdi}\dot{y}_i\right)^2 + \left(v\wedge_{zdi}\dot{y}_i - v\wedge_{ydi}\dot{z}_i\right)^2 + \left(v\wedge_{xdi}\dot{y}_i - v\wedge_{ydi}\dot{x}_i\right)^2}}{\hat{v}_{xdi}\dot{x}_i + \hat{v}_{ydi}\dot{y}_i + \hat{v}_{zdi}\dot{z}_i},
\end{aligned} \tag{40}$$

which implies that $\tilde{\psi}_i(t) = -\arctan 2(\sin(\tilde{\psi}_i(t)), \cos(\tilde{\psi}_i(t)))$. Therefore, the desired yaw angle can be obtained by the following expression:

$$\psi_{di} = \psi_i \underbrace{-\arctan 2(\sin(\tilde{\psi}_i(t)), \cos(\tilde{\psi}_i(t)))}_{\tilde{\psi}_i(t)} \tag{41}$$

Note also that the time derivative of $\tilde{\psi}$ can be calculated as indicated in (43). Therefore, we can write

$$\dot{\psi}_{di} = \dot{\psi}_i + \dot{\tilde{\psi}}_i = \frac{\sin\phi_i}{\cos\theta_i}\omega_{yi} + \frac{\cos\phi_i}{\cos\theta_i}\omega_{zi} + \dot{\tilde{\psi}}_i = \frac{\sin\phi_i}{\cos\theta_i}\omega_{yi} + \frac{\cos\phi_i}{\cos\theta_i}\alpha_{\tilde{\psi}i} + \gamma_{\omega i}(\phi_i, \theta_i)\Omega_{ei} + \dot{\tilde{\psi}}_i, \tag{42}$$

$$\begin{aligned}
S_i &= \sqrt{\left(v\wedge_{xdi}\dot{y}_i - v_{ydi}\dot{x}_i\right)^2 + \left(v\wedge_{zdi}\dot{y}_i - v\wedge_{ydi}\dot{z}_i\right)^2 + \left(v\wedge_{ydi}\dot{z}_i - v\wedge_{zdi}\dot{y}_i\right)^2},\\
Q_i &= 2\left(\hat{v}_{zdi}\dot{y}_i - \hat{v}_{ydi}\dot{z}_i\right)\left(-\dot{z}_i\dot{\hat{v}}_{ydi} - \hat{v}_{ydi}\dot{z}_i + \dot{y}_i\dot{\hat{v}}_{zdi} + \hat{v}_{zdi}\ddot{y}_i\right) + 2\left(\hat{v}_{ydi}\dot{z}_i - \hat{v}_{zdi}\dot{y}_i\right)\left(\dot{z}_i\dot{\hat{v}}_{ydi} + \hat{v}_{ydi}\ddot{z}_i - \dot{y}_i\dot{\hat{v}}_{zdi} - \hat{v}_{zdi}\dot{y}_i\right),\\
\dot{\tilde{\psi}}_i(t) &= -\frac{\hat{v}_{xdi}\dot{x}_i + \hat{v}_{ydi}\dot{y}_i + \hat{v}_{zdi}\dot{z}_i\left(2\left(\hat{v}_{xdi}\dot{y}_i - \hat{v}_{ydi}\dot{x}_i\right)\left(\dot{y}_i\dot{\hat{v}}_{xdi} + \hat{v}_{xdi}\ddot{y}_i - \dot{x}_i\dot{\hat{v}}_{ydi} - \hat{v}_{ydi}\dot{x}_i\right) + Q_i\right)}{2S_i\left(\left(v\wedge_{xdi}\dot{x}_i + v\wedge_{ydi}\dot{y}_i + v\wedge_{zdi}\dot{z}_i\right)^2 + \left(v\wedge_{ydi}\dot{y}_i - v\wedge_{ydi}\dot{x}_i\right)^2 + \left(v\wedge_{ydi}\dot{y}_i - v\wedge_{ydi}\dot{z}_i\right)^2 + \left(v\wedge_{ydi}\dot{z}_i - v\wedge_{zdi}\dot{y}_i\right)^2\right)}\\
&\quad - \frac{S_i\left(\dot{x}_i\dot{\hat{v}}_{xdi} + \hat{v}_{xdi}\dot{x}_i + \dot{y}_i\dot{\hat{v}}_{ydi} + \hat{v}_{ydi}\dot{y}_i + \dot{z}_i\dot{\hat{v}}_{zdi} + \hat{v}_{zdi}\dot{z}_i\right)}{\left(v\wedge_{xdi}\dot{x}_i + v\wedge_{ydi}\dot{y}_i + v\wedge_{zdi}\dot{z}_i\right)^2 + \left(v\wedge_{ydi}\dot{y}_i - v\wedge_{ydi}\dot{x}_i\right)^2 + \left(v\wedge_{ydi}\dot{y}_i - v\wedge_{ydi}\dot{z}_i\right)^2 + \left(v\wedge_{ydi}\dot{z}_i - v\wedge_{zdi}\dot{y}_i\right)^2},
\end{aligned} \tag{43}$$

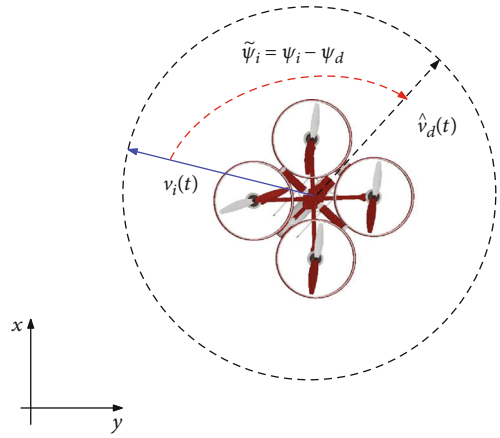

Figure 2: Planar projection of the quadrotor's velocity and the desired velocity generated by the guidance system.

where $\Omega_{ei} = \Omega_i - \alpha_i$ is the angular velocity error, with $\alpha_i = [\alpha_{\tilde{\phi i}}, \alpha_{\tilde{\theta i}}, \alpha_{\tilde{\psi} i}]^\top$ yet to be determined later. $\gamma_{\omega i}(\phi_i, \theta_i) = [00 (\cos\phi_i/\cos\theta_i)]$ and $\alpha_{\tilde{\psi} i}$ is the stabilizing function, which will be chosen such that it cancels out unneeded terms in (42). As such, the stabilizing function can be chosen as follows:

$$\alpha_{\tilde{\psi} i} = \frac{\cos\theta_i}{\cos\phi_i}\left(-\frac{\sin\phi_i}{\cos\theta_i}\omega_{yi} - \dot{\tilde{\psi}}_i + \dot{\psi}_i + \kappa_1\tilde{\psi}_i\right), \tag{44}$$

where κ_1 is a positive gain. Substituting (44) into (42) results in the following closed-loop dynamics:

$$\dot{\tilde{\psi}}_i = -\kappa_1\tilde{\psi}_i + \Upsilon_{\omega i}(\phi_i, \theta_i)\Omega_{ei}. \tag{45}$$

Clearly, if the last term of (45) is exponentially vanishing, then the tracking error $\tilde{\psi}_i$ is also exponentially stable; this can be seen by associating the quadratic Lyapunov function $V_{\psi_i} = (1/2)\tilde{\psi}_i^2$, whose time derivative along the solutions of (45) gives

$$\begin{aligned}\dot{V}_{\psi_i} &= -\kappa_1\tilde{\psi}_i^2 + \gamma_{\omega i}(\phi_i, \theta_i)\tilde{\psi}_i\Omega_{ei} \\ &= -\bar{\kappa}\tilde{\psi}_i^2, \quad \forall|\tilde{\psi}_i| > \sqrt{\frac{1}{2\bar{\kappa}}}\|\gamma_{\omega i}(\phi_i, \theta_i)\Omega_{ei}\|,\end{aligned} \tag{46}$$

where $\bar{\kappa} = \kappa_1 - 1/2 > 0$. Hence, the virtual control law (44) renders the closed-loop (45) system input-to-state stability (ISS) from $\gamma_{\omega i}(\phi_i, \theta_i)\Omega_{ei}$ to $\tilde{\psi}_i$. Therefore, if Ω_{ei} is globally exponentially stable GES, then so is $\tilde{\psi}_i$.

Remark 9. It has been shown in [42] that overturn of the quadrotor can only be avoided if the last component of $\mathbf{R}_i e_z = [\rho_i^m]^\top$, $m = 1 \cdots 3$ (i.e., $\rho_i^m = \cos\theta_i \cos\phi_i$) is ensured to be strictly positive. This constraint further requires that $e_{\zeta i} = \zeta_i - \zeta_{di}$ (with $\zeta_i = [\rho_i, m]^\top$, $m = 1, 2$, and $\zeta_d = [\rho_d, m]^\top$, $m = 1, 2$, is a vector that contains the first two component of $\mathbf{R}_d e_z$) exponentially decays to zero in order to guarantee that $\theta_i \longrightarrow \theta_d$ and $\phi_i \longrightarrow \phi_d$ exponentially. Since $\rho_{i,3} = \sqrt{1 - \rho_{i,1}^2 - \rho_{i,2}^2}$, it is sufficient to show through an adequate control law that $\|\zeta_i\| \leq 1$.

Remark 10. The virtual control (44) is well defined as long as $\theta_i, \phi_i \neq \pi/2$; this singularity is avoided as long as the term $\cos\theta\cos\phi$ is strictly positive or alternatively $\|\zeta_i\| \leq 1$.

Step 2. Controlling the pitch and roll angles.

The pitch and roll angles are contained in the column vector $\mathbf{R}_i e_z$ and are denoted by the vector ζ_i. The time derivative of ζ_i along the solutions of the first equation of (9) and (5) gives the following dynamics:

$$\dot{\zeta}_i = \mathbf{A}_i(\Theta_i)\omega_{i,xy} = \mathbf{A}_i(\Theta_i)\alpha_{i,xy} + [\mathbf{A}_i(\Theta_i), 0_{2\times 1}]\Omega_{ei}, \tag{47}$$

(Θ_i) can be obtained by a long but simple calculation as

$$\mathbf{A}_i(\Theta_i) = \begin{bmatrix} \sin\psi_i\cos\phi_i - \cos\psi_i\sin\theta_i\sin\phi_i & \cos\psi_i\cos\theta_i \\ -\cos\phi_i\cos\psi_i - \sin\phi_i\sin\theta_i\sin\psi_i & \sin\psi_i\cos\theta_i \end{bmatrix}. \tag{48}$$

The matrix $\mathbf{A}_i(\Theta_i)$ is invertible, due to the fact that $\det(\mathbf{A}_i(\Theta_i)) = 1/\cos\theta_i\cos\phi_i$, which implies that as long as the singularity (i.e., $\theta_i = \phi_i = \pi_i/2$) is avoided, the matrix is nonsingular. The control objective is therefore to ensure on top of forcing the pitch and roll angles to track their immediate desired values and to also prevent them from violating the constraint that leads to singularity. In other words, the state variable ζ_i is required to remain in the set $\|\zeta_i\| < 1$ for all $t \geq 0$. To address this problem, the integral barrier Lyapunov function iBLF [29] will be employed to guarantee nonviolation of the aforementioned constraint.

Motivated by the work in [29], in order to design the virtual control $\omega_{i,xy}$, the following integral barrier Lyapunov candidate functional is proposed:

$$V_{\zeta i}(\zeta_{ei}(t), \zeta_d(t)) = \int_0^{\zeta_{ei}} \frac{\sigma_i^\top}{1 - (\sigma_i + \zeta_d)^\top(\sigma_i + \zeta_d)}\, d\sigma_i, \tag{49}$$

where $\zeta_{ei} = \zeta_i - \zeta_d$. It can be seen that $V_{\zeta i}(\zeta_{ei}(t), \zeta_d(t))$ is positive definite and continuously differentiable and satisfies the decrescent condition in the set $\|\zeta_i\| < 1$ such that for $\sigma_i = \eta_i\zeta_{ei}$, we have

$$\begin{aligned}\frac{1}{2}\zeta_{ei}^\top\zeta_{ei} &< V_{\zeta_i}(\zeta_{ei}(t), \zeta_d(t)) \\ &< \zeta_{ei}^\top\zeta_{ei}\int_0^1 \frac{\eta_i}{1 - (\eta_i\zeta_{ei} + \zeta_d)^\top(\eta_i\zeta_{ei} + \zeta_d)}\, d\eta_i.\end{aligned} \tag{50}$$

Based on the definition in (49), the time derivative of the iBLF $V_{\zeta i}(\zeta_{ei}(t), \zeta_d(t))$ along the solutions of (47) yields

$$\dot{V}_{\zeta i}(\zeta_{ei}(t), \zeta_d(t)) = \frac{\zeta_{ei}^\top}{1-\zeta_i^\top\zeta_i}\left(\mathbf{A}_i(\Theta_i)\alpha_{i,xy} + [\mathbf{A}_i(\Theta_i), 0_{2\times 1}]\Omega_{ei}\right) + \left(\frac{\partial V_{\zeta i}}{\partial \zeta_d}\right)^\top \dot{\zeta}_d, \tag{51}$$

where $\partial V_{\zeta i}/\partial\zeta_d = (\zeta_{ei}^\top/(1-\zeta_i^\top\zeta_i) - \chi_i(\zeta_i, \zeta_d))\zeta_i$ and $\chi_i(\zeta_i, \zeta_d) = \int_0^1(\eta_i\zeta_{ei}+\zeta_d)^\top 1/(1-(\eta_i\zeta_{ei}+\zeta_d)^\top(\eta_i\zeta_{ei}+\zeta_d))d\eta_i$ with the vector 1 being all components 1. We can obtain the stabilizing function $\alpha_{i,xy}$ as

$$\alpha_{i,xy} = \mathbf{A}_i(\Theta_i)^{-1}\left(-\kappa_2\zeta_{ei} + (1-\zeta_i)^\top(1-\zeta_i)\chi_i\dot{\zeta}_d\right), \tag{52}$$

where κ_2 is a positive gain to be designed. Under (52), the time derivative of $V_{\zeta i}$ is given by

$$\dot{V}_{\zeta i} = \frac{-\kappa_2\zeta_{ei}^\top\zeta_{ei}}{1-\zeta_i^\top\zeta_i} + \frac{\zeta_{ei}^\top}{1-\zeta_i^\top\zeta_i}[\mathbf{A}_i(\Theta_i), 0_{2\times 1}]\Omega_{ei}, \tag{53}$$

at this step according to (53); the time derivative of $V_{\zeta i}$ becomes negative definite only when Ω_{ei} exponentially converges to zero. The design of the force moment is not finished yet. One more step is required to ensure that Ω_{ei} exponentially converges to zero.

Step 3. Force moment control design.

The angular velocity error dynamics Ω_{ei} based on the second equation of (9) has the following form:

$$Ji\dot{\Omega}_{ei} = J\dot{\Omega}_i - Ji\dot{\alpha}_i = -\Omega_i \times J_i\Omega_i + \tau_i + \Delta_{\Omega i} - J\dot{\alpha}_i. \tag{54}$$

At this stage, the control input for the force moment τ_i can be readily designed to compensate for the coupling terms created in the previous steps and the external perturbation to which the quadrotor is subject. To this end, let the control input be designed as follows:

$$\begin{aligned}
\tau_i &= -\mathbf{K}_i\Omega_{ei} + J_i\dot{\alpha}_i + \Omega_i \times J_i\Omega_i - \Upsilon\omega i(\phi_i, \theta_i)^\top\tilde{\psi}_i \\
&\quad - [\mathbf{A}_i(\Theta_i), 0_{2\times 1}]^\top\frac{\zeta_{ei}}{1-\zeta_i^\top\zeta_i} - \widehat{\Delta}_{\Omega_i}, \\
\widehat{\Delta}_{\Omega_i} &= \varrho\Omega_i + K_{\Omega_i}\Omega_i, \\
\dot{\varrho}\Omega_i &= -K_{\Omega_i}\varrho_{\Omega_i} - K_{\Omega_i}\left(-\Omega_i \times J_i\Omega_i + \tau_i + \Delta_{\Omega_i} + K_{\Omega_i}\varrho\right),
\end{aligned} \tag{55}$$

where $\mathbf{K}_i$ is a diagonal positive gain matrix and K_Ω is a symmetric and positive definite matrix.

Remark 11. The disturbance term is compensated for by an estimate $\widehat{\Delta}_{\Omega_i}$ which is the output of a nonlinear-observer inspired by [40]. The particularity of this type of observer is to guarantee an exponential convergence of the unknown disturbance to its true value. Furthermore, as we want the inner control loop (i.e., attitude dynamics) to be fast convergent as compared to the dynamic behavior of the outer control loop (i.e., translational dynamics), our choice is hence justified by ensuring complete cancellation of the uncertain terms.

For the convenience of stability analysis, we apply the control input (55) along with the virtual controls (52) and (44) and then the error attitude dynamics becomes

$$\begin{aligned}
\dot{\tilde{\psi}}_i &= -\kappa_1\tilde{\psi}_i + \gamma_{\omega i}(\phi_i, \theta_i)\Omega_{ei}, \\
\dot{\zeta}_{ei} &= -\kappa_2\zeta_{ei} + (1-\zeta_i)^\top(1-\zeta_i)\chi_i\dot{\zeta}_d + [\mathbf{A}_i(\Theta_i), 0_{2\times 1}]\Omega_{ei}, \\
J\dot{\Omega}_{ei} &= -\mathbf{K}_i\Omega_{ei} - \gamma_{\omega i}(\phi_i, \theta_i)^\top\tilde{\psi}_i - [\mathbf{A}_i(\Theta_i), 0_{2\times 1}]^\top\frac{\zeta_{ei}}{1-\zeta_i^\top\zeta_i} \\
&\quad - \tilde{\Delta}_{\Omega_i},
\end{aligned} \tag{56}$$

$$\widehat{\Delta}_{\Omega i} = \varrho_{\Omega i} + K_{\Omega i}J_i\Omega_i, \tag{57}$$

$$\dot{\varrho}\Omega_i = -K_{\Omega i}\varrho_{\Omega i} - K_{\Omega i}(-\Omega_i \times J_i\Omega_i + \tau_i + K_{\Omega i}\Omega_i). \tag{58}$$

The control design for the attitude inner-loop dynamics has been completed. We summarize the results in the following proposition.

Proposition 12. *Consider the attitude dynamics (9), given a desired attitude $\mathbf{R}_d e_z$ extracted from the positioning controller (31), under the proposed attitude control (55), the error vector $\Xi_i = [\tilde{\psi}_i, \zeta_{ei}^\top, \Omega_{ei}^\top, \tilde{\Delta}_{\Omega i}^\top]^\top$ of the attitude dynamics described by equations (56) and (57) is exponentially stable for any initial condition $\Xi_i(t_0) \in Q_i$, where $Q_i = \mathbb{R}\times\mathcal{Z}_i\times\mathbb{R}^3\times\mathbb{R}^3$ and $Z_i = \{\zeta_i \in \mathbb{R}_3 : \|\zeta_i\| \le 1\}$. In particular, for any initial condition $\zeta_i(t_0) \in Z_i$, the constraint $\|\zeta_i(t)\| < 1$ is satisfied $\forall t > 0$.*

Proof. The stability analysis of the attitude dynamics is conducted by considering the following Lyapunov function of the associated attitude variables:

$$V_{AT}^i = V_{\psi i} + V_{\zeta i} + \frac{1}{2}\Omega_{ei}^\top J_i\Omega_{ei} + \frac{\delta_0}{2}\tilde{\Delta}_{\Omega i}^\top\tilde{\Delta}_{\Omega i}, \tag{59}$$

where δ_0 is a positive constant to be determined later. Differentiating both side of (59) along the solutions of

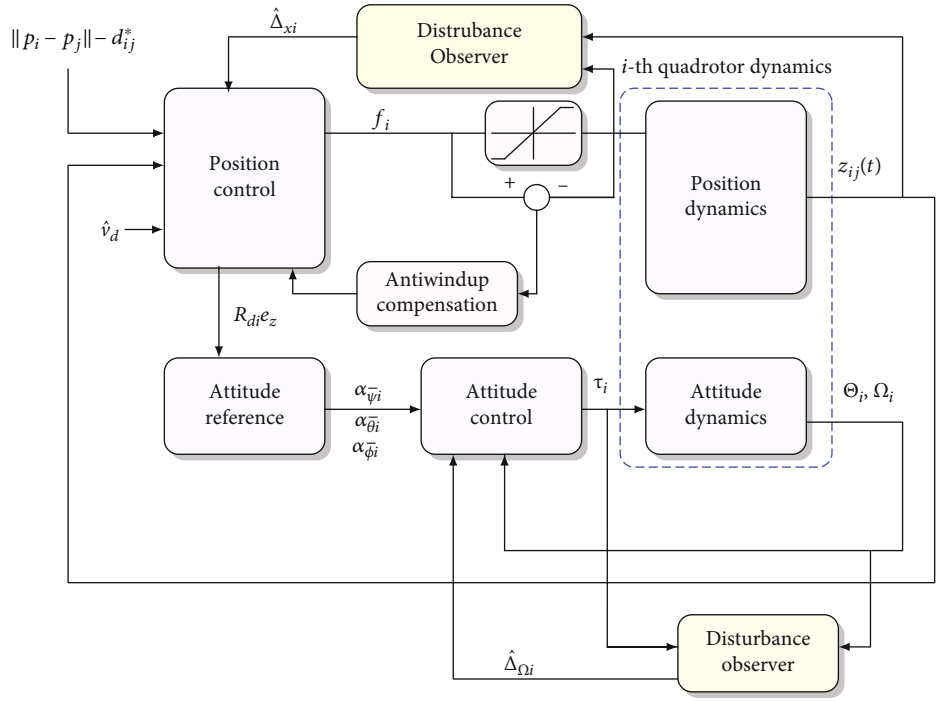

Figure 3: Block diagram of the decentralized distance-based formation control.

the closed-loop system consisting of (56) and (57) gives

$$\begin{aligned}
\dot{V}_{AT}^{i} &= \dot{V}_{\psi i} + \dot{V}_{\zeta i} + \Omega_{ei}^{\top} J_i \dot{\Omega}_{ei} + \delta_0 \tilde{\Delta}_{\Omega i}^{\top} \dot{\tilde{\Delta}}_{\Omega i} \\
&= -\kappa_1 \tilde{\psi}_i^2 - \frac{\kappa_2 \zeta_{ei}^{\top} \zeta_{ei}}{1 - \zeta_i^{\top} \zeta_i} + \frac{\zeta_{ei}^{\top}}{1 - \zeta_i^{\top} \zeta_i} [\mathbf{A}_i(\Theta_i), 0_{2\times 1}] \Omega_{ei} \\
&\quad + \gamma_{\omega i}(\phi_i, \theta_i) \tilde{\psi}_i \Omega_{ei} + \Omega_{ei}^{\top} \left(-\mathbf{K}_i \Omega_{ei} - \gamma_{\omega i}(\phi_i, \theta_i)^{\top} \tilde{\psi}_i \right. \\
&\quad \left. - [\mathbf{A}_i(\Theta_i), 0_{2\times 1}]^{\top} \frac{\zeta_{ei}}{1 - \zeta_i^{\top} \zeta_i} - \tilde{\Delta}_{\Omega_i} \right) - \delta_0 \tilde{\Delta}_{\Omega i}^{\top} \hat{\tilde{\Delta}}_{\Omega i} \\
&= -\kappa_1 \tilde{\psi}_i^2 - \frac{\kappa_2 \zeta_{ei}^{\top} \zeta_{ei}}{1 - \zeta_i^{\top} \zeta_i} - \Omega_{ei}^{\top} \mathbf{K}_i \Omega_{ei} - \Omega_{ei}^{\top} \tilde{\Delta}_{\Omega_i} - \delta_0 \tilde{\Delta}_{\Omega i}^{\top} K_{\Omega i} \tilde{\Delta}_{\Omega_i} \\
&\le -\kappa_1 \tilde{\psi}_i^2 - \frac{\kappa_2 \zeta_{ei}^{\top} \zeta_{ei}}{1 - \zeta_i^{\top} \zeta_i} - \underbrace{\left(\lambda_{\min}(\mathbf{K}_i) - \frac{1}{2} \right)}_{k_{0i}} \|\Omega_{ei}\|^2 \\
&\quad - \underbrace{\left(\delta_0 \lambda_{\min}(K_{\Omega i}) - \frac{1}{2} \right)}_{k_{1i}} \left\| \tilde{\Delta}_{\Omega i} \right\|^2.
\end{aligned} \tag{60}$$

In light of the last inequality in (60) and in order to ensure that $\dot{V}_{AT}^{i}$ is negative definite, one can select the matrix $\mathbf{K}_i$ such that $\lambda_{\min}(\mathbf{K}_i) > 1/2$. Also, the observer gain $K_{\Omega i}$ is selected such that $\lambda_{\min}(K_{\Omega i}) > 2(1/\delta_0)$, where δ_0 can always be picked as a sufficiently small constant. Note, however, that δ_0 is not needed in the implementation of the proposed controller.

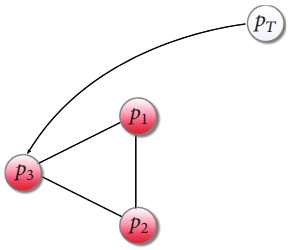

Figure 4: A minimally rigid undirected graph adopted for simulations.

Now referring to Lemma 2 in [29] to approximate the functional $V_{\zeta i}$, it is shown that for all $\|\zeta_i(t)\| \le 1$, the following inequality holds:

$$V_{\zeta_i} \le \frac{\zeta_{ei}^{\top} \zeta_{ei}}{1 - \zeta_i^{\top} \zeta_i}. \tag{61}$$

Based on (61), the inequality (60) rewrites

$$\dot{V}_{AT}^{i} \le -2_{\kappa_1} V_{\psi i} - \kappa_2 V_{\zeta i} - k_{0i} \|\Omega_{ei}\|^2 - k_{1i} \left\| \tilde{\Delta}_{\Omega i} \right\|^2 \le -\beta_i V_{AT}^{i}, \tag{62}$$

where $\beta_i := \min\{2\kappa_1, 2\kappa_2, 2(k_2/\|J_i\|), 2(k_2/\delta_0)\}$. It implies that

$$\|\Xi_i(t)\| \le \sqrt{2 V_{AT}^{i}(0) e^{-\beta_i t/2}}, \tag{63}$$

where $\Xi_i(t) = [\tilde{\psi}_i, \zeta_i^{\top}, \Omega_{ei}^{\top}, \tilde{\Delta}_{\Omega i}^{\top}]^{\top}$. This implies that the closed-loop system (56) and (57) is locally exponentially stable at the

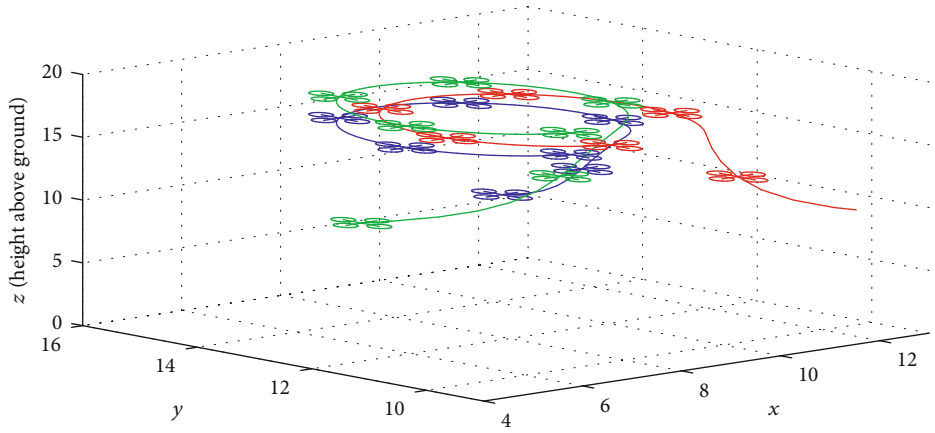

Figure 5: 3D position trajectory of the three quadrotors.

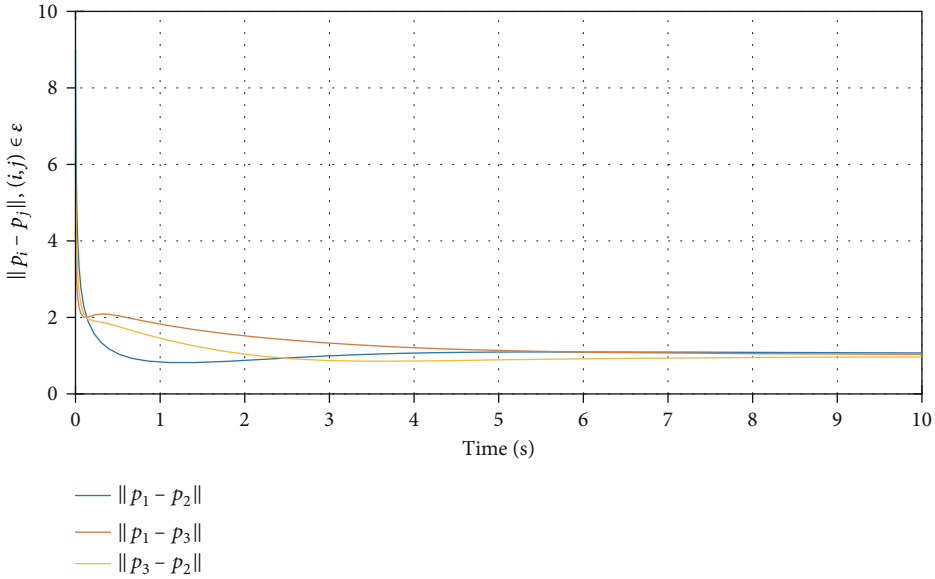

Figure 6: Distance errors.

origin. Furthermore, it can be seen that $\|\zeta_i\|$ is bounded by an exponentially decreasing function. Then, from (61), it can be concluded that $V_{\zeta i}$ is also bounded by an exponentially decreasing function such that $V_{\zeta i} \leq c_{0i}$ with $c_{0i} \coloneqq 2V_{ATi}(0)$. On the other hand, since by construction $V_{\zeta i} \longrightarrow \infty$ as $\|\zeta_i\| \longrightarrow 1$, it can be inferred from the fact that $V_{\zeta i}$ is bounded for all $t \geq 0$ and the state $\zeta_i(t)$ always satisfies the constraint $|\zeta_i(t)\| \leq 1$, provided that $\|\zeta_i(0)\| \leq 1$. This completes the proof.

Remark 13. The controller τ_i in (55) involves the derivative of the virtual control α_i, which appears to be difficult to calculate. So the robust differentiator [43] can be introduced to handle finite convergence of $\dot{\alpha}_i$ to its true value.

5. Control Law Synthesis: Closed-Loop System Stability Analysis

Before moving on to the stability analysis, we summarize as follows the motion control hierarchy developed in this work. First, a decentralized formation controller is designed for the open-loop translational dynamics of each individual quadrotor, which is based only on exchanging the relative position among neighbor quadrotors to guarantee safe formation maneuver and target interception. Second, the flight controller of the individual quadrotor receives the appropriate signal commands and ensures the relevant aerodynamic thrust and desired attitude necessary to achieve track-following of the leader whose only available information is its position. The resulting guidance and inner- and outer-loop control structures are illustrated in Figure 3.

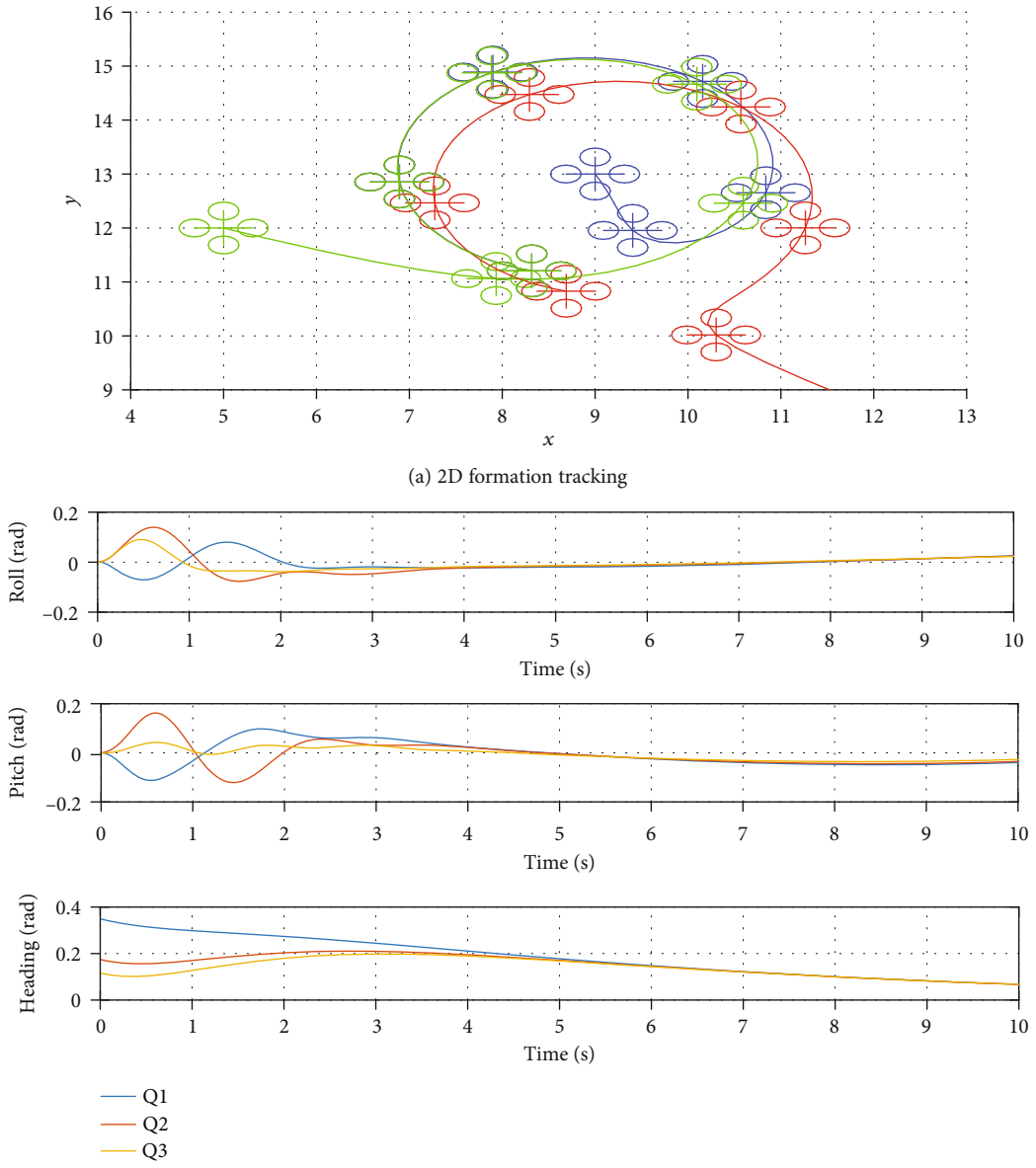

(a) 2D formation tracking

(b) Velocity tracking errors

Figure 7: Convergence of the backstepping state tracking errors.

The total motion control system can now be analyzed by considering the complete system composed of the decentralized controller for the translational dynamics (15) and the orientation dynamics (56)–(57). The main result is presented in the following theorem:

Theorem 14. *Consider a group of n quadrotors each of which is described by the dynamics (7)–(9). If the set of quadrotors are organized at an initial minimally and infinitesimally rigid configuration, Assumptions 5 and 6 hold, and if the initial conditions for the roll and pitch angles are away from the singularity angles (i.e., $\pi/2$), then the decentralized control law and update laws consisting of (30), (31), (27), and (28) along with the constrained attitude control (55) guarantee achievement of the control objectives (13) and (14). In particular, the combined closed-loop inner- and outer-loop dynamics are forward complete, and the origin of the whole system is GAS.*

Proof. The closed-loop of the overall system consists of the translational and the rotational dynamics of the n quadrotor in the formation group. In previous sections, each subsystem has been treated separately to investigate its stability property, assuming the interconnection terms among the subsystems are neglected. In this proof, the closed-loop system is rewritten with their corresponding interconnected terms:

$$\Sigma_X : \begin{cases} \dot{X} = F\left(z, \bar{v}_e, \tilde{\Delta}_x\right) + H_e(t, X)\bar{\zeta}_e, \\ y_1 = \bar{v}_e, \end{cases} \tag{64}$$

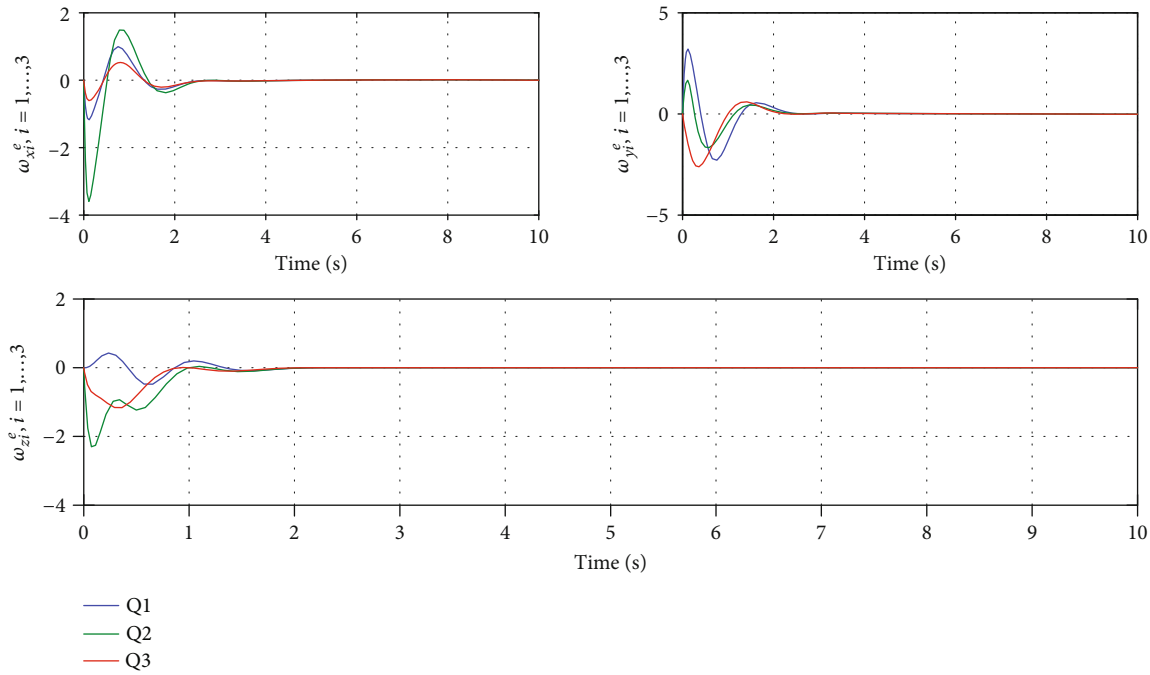

Figure 8: Angular velocity errors.

$$\Sigma_{\bar{\psi}}: \begin{cases} \dot{\bar{\Xi}} = G\left(\bar{\Xi}, \tilde{\Delta}_{\Omega}, \bar{\zeta}_e\right), \\ y_2 = \bar{\zeta}_e, \end{cases} \tag{65}$$

where $X = [z^\top, \bar{v}_e^\top]^\top$, $H_e(t,z) = [O_{3\times n}|\text{diag}\,(f_1, f_2, \cdots, f_n)]$, $\bar{\zeta}_e = [0_{1\times n}^\top, \zeta_{e1}^\top, \cdots, \zeta_{en}^\top]^\top$. Systems (64) and (65) can be viewed as a cascaded decomposition of two subsystems, where the cooperative translational dynamics are viewed as perturbed nominal systems where the perturbation terms are driven by the attitude dynamics subsystems. In order to proceed with the stability analysis of the cascaded subsystems, it is first necessary to prove that the solutions of the whole systems do not escape to infinity in a finite time. One way to show that is to prove forward completeness [44] of the closed-loop systems (64) and (65).

Consider the following Lyapunov function:

$$V_f = V_2 + \sum_{i=1}^{n} V_{AT}^i. \tag{66}$$

Taking the time derivative of V_f along the closed-loop systems (56) and (57) yields

$$\begin{aligned} \dot{V}_f &= \dot{V}_2 + \sum_{i=1}^{n} \dot{V}_{AT}^i = a_z V_2 + X^\top H_e(t,X)\bar{\zeta}_e - \sum_{i=1}^{n} \beta_i V_{AT}^i \\ &\le a_z V_2 + \frac{1}{2}\|X\|^2\|H_e(t,X)\|^2 + \frac{1}{2}\left\|\bar{\zeta}_e\right\|^2 + \bar{\beta}\sum_{i=1}^{n} V_{AT}^i \\ &\le a_z V_2 + \left(\bar{\beta}+1\right)\sum_{i=1}^{n} V_{AT}^i + \frac{1}{2}\|X\|^2\|H_e(t,X)\|^2 \\ &\le C_0 V_f + \sigma(\|X\|), \end{aligned} \tag{67}$$

where $\bar{\beta} = \min\ \{\beta_i\}$, $i = 1, \cdots n$; C_0 is a positive constant; and $\sigma(.)$ is a class-K_∞ function. Hence, according to [44], the closed-loop systems (56) and (57) are forward complete. This result implies that we can proceed and analyze the overall system as a cascaded system. Note from (64), it can easily be verified that $F(0,0,0) = 0$. Furthermore, to show steadiness of systems (64) and (65), it is sufficient to show that both conditions in Lemma 4 are satisfied. Clearly, from previous sections, we showed that the nominal system Σ_X (without the coupling term) is locally exponentially stable (LES), also for the subsystem $\Sigma_{\bar{\psi}}$. The fact that these two cascaded subsystems are LES is because the term $\|H_e(t,X)\bar{\zeta}_e\|$ verifies the linear growth condition (2). Indeed, it is easy to figure out that the coupling term satisfies

$$H_e(t,X)\bar{\zeta}_e \le \|H_e(t,X)\|\left\|\bar{\Xi}\right\| \le \underbrace{\left(\sum_{i=1}^{n} f_i^2\right)^{1/2}}_{\gamma(z)}\left\|\bar{\Xi}\right\|. \tag{68}$$

Furthermore, taking $V_2 = W$, it can be easily shown that conditions (3) are satisfied. This completes the stability analysis of the cascaded subsystems.

6. Numerical Simulations

To show the effectiveness of the proposed constrained distance-based formation controller for a group of quadrotors, numerical simulations are carried out in this section using the MATLAB software platform. In order to make the simulation close to reality, a Gaussian white noise is added to the measured signals including distance measurements among neighboring quadrotors, local velocity, and attitude using rand (.) function. In the simulation, we

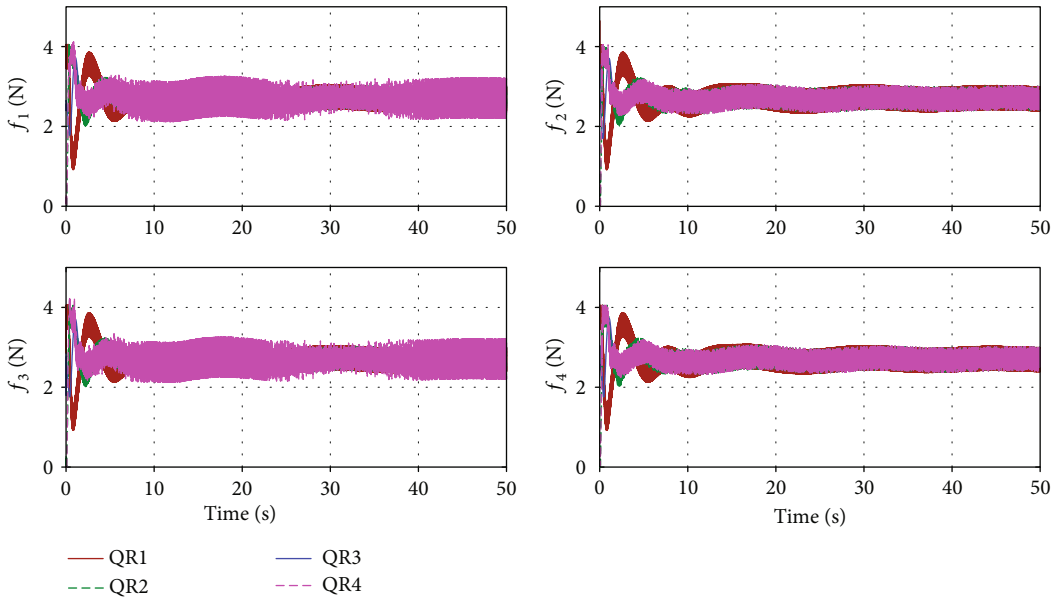

Figure 9: Thrust force.

consider three quadrotors, where a reference trajectory is only known by the leader in the group as shown in Figure 4. In this configuration, all quadrotors are equidistantly distributed around the leader, such that $d_{ij}^{\star} = 1$ m. For the simulations, the quadrotor follower system parameters are selected as $m_i = 8.2$ kg, the inertia moment is $J_i = \text{diag}\,(0.18, 0.34, 0.28)\ \text{kg} \cdot \text{m}^2$, and we assumed $g = 9.8\ \text{m/s}^2$. The initial conditions for the quadrotor followers are taken as $\mathbf{p}_{1f}(0) = [-5, -2, 0]^{\top}$, $\mathbf{p}_{2f}(0) = [10, 3, 4]^{\top}$, $\mathbf{p}_{3f}(0) = [10, 3, 4]^{\top}$, $v_{\text{if}}(0) = [0, 0, 0]^{\top}$, and $\Omega_{\text{if}}(0) = [0, 0, 0]^{\top}$ where the subscript if stands for follower vehicle $i = 1, \cdots, 3$. The initial values of $\Theta_i(0)$ are chosen such that $[\phi_i(0), \theta_i(0), \psi_i(0)]^{\top} = [4, -2, 1]^{\top}(\pi/3i)$, $i = 1, \cdots, 3$. The initial values chosen for the roll and pitch angles, $\phi_i(0)$ and $\theta_i(0)$, $i = 1, \cdots, 3$, respectively, are to illustrate the ability of the proposed formation control design to handle large roll and pitch angles without violating the constraints that lead to singularity. The target reference trajectory and the desired heading of the leader quadrotor are chosen as follows:

$$\begin{cases} \mathbf{p}_T(t) = \begin{pmatrix} 2\sin(0.3t) \\ 2 - 2\cos(0.3t) \\ 10 - 10e^{-0.4t} \end{pmatrix}, \\ \psi_d = 0.2e^{-0.5t}. \end{cases} \tag{69}$$

To test the robustness of the controller, external disturbances acting on the quadrotor due to wind have been added, which can be modelled by the forces $\Delta_{xi} = [1 + 0.5\cos(2t), 1 + 0.5\cos(2t), 0.5\cos(2t)]^{\top}$ and $\Delta_{\Omega i} = [0.5 + 0.5\sin(2t), 1.5 + 0.2\sin(2t), 0.1\sin(2t)]^{\top}$. The control gain parameters for the translational dynamics are $k = 10$, $k_{1i} = 5$, $k_{2i} = 15$, $\mathbf{K}_{\xi i} = 7$, $\mathbf{K}_{xi} = 15$. The safety distance before collision and connectivity range specifications are set according to the performance parameters $\bar{\ell}_0 = 0.5$, $\underline{\ell}_{\infty} = 1$ m, and $a = 0.1$. The control gains for the attitude dynamics are chosen such that $\kappa_1 = 10$, $\kappa_2 = 15$, $\mathbf{K}_i = \text{diag}\,(10,10,10)$, and $K_{\Omega i} = \text{diag}\,(5, 5, 5)$.

Figure 5 shows the evolution of the three-dimensional position of three quadrotors following the reference trajectory. It can be seen that the proposed controller provides global asymptotic convergence towards the reference trajectory. This can also be verified in Figure 6, where it can be shown how the distance between quadrotors asymptotically converges to the prescribed fixed value. Figure 7 corroborates these results through the convergence of the attitude angles to their desired values. Clearly, the attitude angles of all quadrotors in the group aggregate on the angular value during the formation. It can also be noticed that the pitch and roll angles are within the authorized range of variation and thus do not allow the quadrotor to overturn during the maneuver. Figure 8 depicts the asymptotic convergence of the angular velocity tracking error to zero, which validates the results of Theorem 14. Finally, the thrust forces and the torques applied to the quadrotors can be seen in Figures 9 and 10. From these plots, it can be concluded that the numerical results illustrate that the leader-follower strategy has a successful tracking performance.

7. Conclusion

In this paper, a strategy for formation maintenance with target interception control of a quadrotor-type aerial vehicle was investigated. The proposed decentralized controller guaranteed formation establishment with prescribed transient and steady state performances while avoiding interagent collision

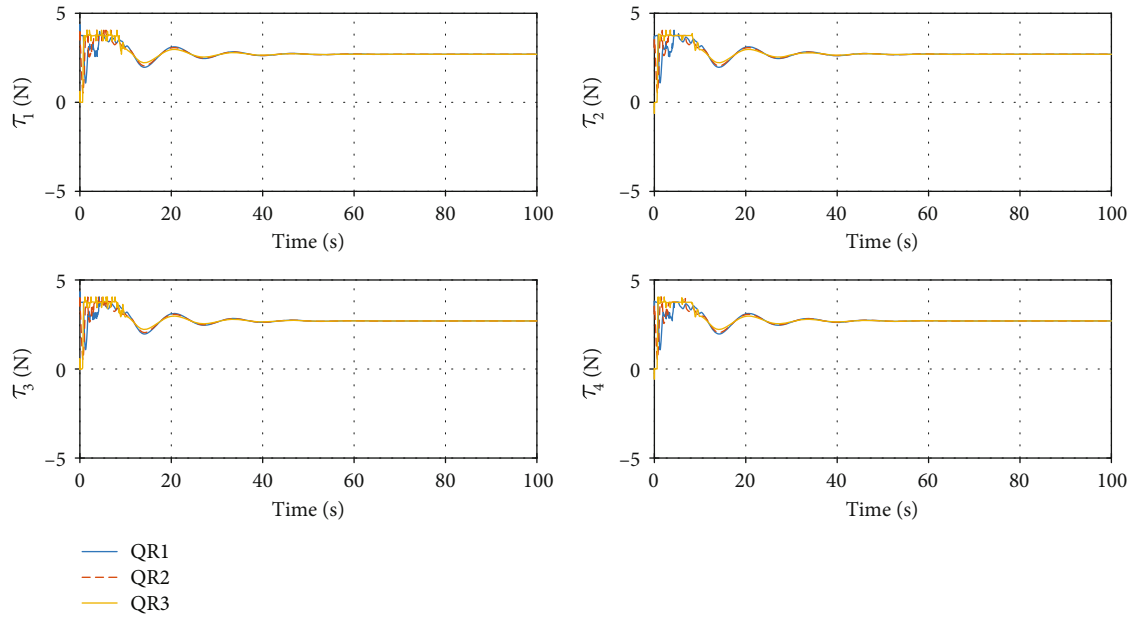

Figure 10: Torque moments.

and connectivity losses. A distinctive feature of the proposed approach is that the group of quadrotors does not need explicit communication exchange; it only relies on the relative position of the neighboring vehicles and local sensor measurements. This makes the proposed decentralized control protocol extremely simple and easy to implement. Furthermore, the integral barrier Lyapunov function and the backstepping technique were instrumental to the implementation of the attitude controller which ensured that the quadrotor avoids overturning during the formation maneuver. The future work is to carry out experiments to test the proposed formation control design.

Data Availability

All the data are in the manuscript that validate the concept of the design.

Conflicts of Interest

The authors declare that they have no conflict of interest.

References

[1] V. Devalla and O. Prakash, "Developments in unmanned powered parachute aerial vehicle: a review," *IEEE Aerospace and Electronic Systems Magazine*, vol. 29, no. 11, pp. 6–20, 2014.

[2] L. Panagiotopoulou, ""Eye in the sky" project - intelligent transport infrastructure for traffic monitoring and mobility information," in *2004 IEEE 59th Vehicular Technology Conference. VTC 2004-Spring (IEEE Cat. No.04CH37514)*, pp. 2926–2930, Milan, Italy, 2004.

[3] P. E. I. Pounds, *Design, Construction and Control of a Large Quadrotor Micro Air Vehicle, [Ph.D. thesis]*, Australian National University, Australia, 2007.

[4] K. Sreenath, T. Lee, and V. Kumar, "Geometric control and differential flatness of a quadrotor UAV with a cable-suspended load," in *52nd IEEE Conference on Decision and Control*, pp. 2226–2274, Florence, Italy, 2013.

[5] T. Tomic, K. Schmid, P. Lutz et al., "Toward a fully autonomous UAV: research platform for indoor and outdoor urban search and rescue," *IEEE Robotics & Automation Magazine*, vol. 19, no. 3, pp. 46–56, 2012.

[6] K. D. Do, "Coordination control of quadrotor VTOL aircraft in three-dimensional space," *International Journal of Control*, vol. 88, no. 3, pp. 543–558, 2014.

[7] F. Fahimi, "Full formation control for autonomous helicopter groups," *Robotica*, vol. 26, no. 2, pp. 143–156, 2008.

[8] L. Garcia-Delgado, A. Dzul, V. Santibanez, and M. Llama, "Quad-rotors formation based on potential functions with obstacle avoidance," *IET Control Theory & Applications*, vol. 6, no. 12, pp. 1787–1802, 2012.

[9] A. P. Mrudula and J. L. Nandagopal, "Line-of-sight guidance for formation control of quadrotor," in *2017 International Conference on Circuit, Power and Computing Technologies (ICCPCT)*, pp. 1–8, Kollam, India, April 2017.

[10] B. Yu, X. Dong, Z. Shi, and Y. Zhong, "Formation control for quadrotor swarm systems: algorithms and experiments," in *Proceedings of the 32nd Chinese Control Conference*, pp. 7099–7104, Xi'an, China, July 2013.

[11] V. Roldão, R. Cunha, D. Cabecinhas, C. Silvestre, and P. Oliveira, "A leader-following trajectory generator with application to quadrotor formation flight," *Robotics and Autonomous Systems*, vol. 62, no. 10, pp. 1597–1609, 2014.

[12] T. Balch and R. C. Arkin, "Behavior-based formation control for multirobot teams," *IEEE Transactions on Robotics and Automation*, vol. 14, no. 6, pp. 926–939, 1998.

[13] S. Monteiro and E. Bicho, "Attractor dynamics approach to formation control: theory and application," *Autonomous Robots*, vol. 29, no. 3-4, pp. 331–355, 2010.

[14] J. Ghommam, L. F. Luque-Vega, B. Castillo-Toledo, and M. Saad, "Three-dimensional distributed tracking control for multiple quadrotor helicopters," *Journal of the Franklin Institute*, vol. 353, no. 10, pp. 2344–2372, 2016.

[15] A. Sadowska, T. . den Broek, H. Huijberts, N. van de Wouw, D. Kostić, and H. Nijmeijer, "A virtual structure approach to formation control of unicycle mobile robots using mutual coupling," *International Journal of Control*, vol. 84, no. 11, pp. 1886–1902, 2011.

[16] R. Wang and J. Liu, "Adaptive formation control of quadrotor unmanned aerial vehicles with bounded control thrust," *Chinese Journal of Aeronautics*, vol. 30, no. 2, pp. 807–817, 2017.

[17] D. Zhou and M. Schwager, "Virtual rigid bodies for coordinated agile maneuvering of teams of micro aerial vehicles," in *2015 IEEE International Conference on Robotics and Automation (ICRA)*, pp. 1737–1742, Seattle, WA, USA, May 2015.

[18] D. Li, S. S. Ge, W. He, G. Ma, and L. Xie, "Multilayer formation control of multi-agent systems," *Automatica*, vol. 109, article 108558, 2019.

[19] Y. Qi, J. Wang, and J. Shan, "Collision-free formation control for multiple quadrotor-manipulator systems*," *IFAC Papers OnLine*, vol. 50, no. 1, pp. 7923–7928, 2017.

[20] A. A. A. Rizqi, A. I. Cahyadi, and T. B. Adji, "Path planning and formation control via potential function for UAV quadrotor," in *2014 International Conference on Advanced Robotics and Intelligent Systems (ARIS)*, pp. 165–170, Taipei, Taiwan, June 2014.

[21] C. Hua, J. Chen, and Y. Li, "Leader-follower finite-time formation control of multiple quadrotors with prescribed performance," *International Journal of Systems Science*, vol. 48, no. 12, pp. 2499–2508, 2017.

[22] D. A. Mercado, R. Castro, and R. Lozano, "Quadrotors flight formation control using a leader-follower approach," in *2013 European Control Conference (ECC)*, pp. 3858–3863, Zurich, Switzerland, July 2013.

[23] E. Kyrkjebo and K. Y. Pettersen, "A virtual vehicle approach to output synchronization control," in *Proceedings of the 45th IEEE Conference on Decision and Control*, San Diego, CA, USA, 2006.

[24] A. Ailon and S. Arogeti, "Formation control strategies for autonomous quadrotor-type helicopters," *IFAC Proceedings Volumes*, vol. 46, no. 30, pp. 324–329, 2013.

[25] T. Dierks and S. Jagannathan, "Guidance laws for autonomous underwater vehicles," in *Aerial Vehicles*, T. M. Lam, Ed., pp. 23–64, I-Tech Education and Publishing, 2009.

[26] H. M. Guzey, T. Dierks, S. Jagannathan, and L. Acar, "Modified consensus-based output feedback control of quadrotor UAV formations using neural networks," *Journal of Intelligent & Robotic Systems*, vol. 94, no. 1, pp. 283–300, 2019.

[27] Z. Hou and I. Fantoni, "Leader-follower formation saturated control for multiple quadrotors with switching topology," in *2015 Workshop on Research, Education and Development of Unmanned Aerial Systems (RED-UAS)*, pp. 8–14, Cancun, Mexico, November 2015.

[28] K.-K. Oh, M.-C. Park, and H.-S. Ahn, "A survey of multi-agent formation control," *Automatica*, vol. 53, pp. 424–440, 2015.

[29] Z.-L. Tang, S. S. Ge, K. P. Tee, and W. He, "Robust adaptive neural tracking control for a class of perturbed uncertain nonlinear systems with state constraints," *IEEE Transactions on Systems, Man, and Cybernetics: Systems*, vol. 99, pp. 1–12, 2016.

[30] P. Castillo, R. Lozano, and A. E. Dzul, *Modelling and Control of Mini-Flying Machines*, Springer-Verlag, Springer, London, 2005.

[31] X. Ding, X. Wang, Y. Yu, and C. Zha, "Dynamics modeling and trajectory tracking control of a quadrotor unmanned aerial vehicle," *Journal of Dynamic Systems, Measurement, and Control*, vol. 139, no. 2, article 021004, 2017.

[32] T.-T. Tran, S. S. Ge, and W. He, "Adaptive control of a quadrotor aerial vehicle with input constraints and uncertain parameters," *International Journal of Control*, vol. 91, no. 5, pp. 1140–1160, 2017.

[33] X. Cai and M. de Queiroz, "Formation maneuvering and target interception for multi-agent systems via rigid graphs," *Asian Journal of Control*, vol. 17, no. 4, pp. 1174–1186, 2015.

[34] F. Kendoul, "Nonlinear hierarchical flight controller for unmanned rotorcraft: design, stability, and experiments," *Journal of Guidance, Control, and Dynamics*, vol. 32, no. 6, pp. 1954–1958, 2009.

[35] L. Asimow and B. Roth, "The rigidity of graphs, II," *Journal of Mathematical Analysis and Applications*, vol. 68, no. 1, pp. 171–190, 1979.

[36] C. P. Bechlioulis and G. A. Rovithakis, "Adaptive control with guaranteed transient and steady state tracking error bounds for strict feedback systems," *Automatica*, vol. 45, no. 2, pp. 532–538, 2009.

[37] C. Wang and Y. Lin, "Decentralized adaptive tracking control for a class of interconnected nonlinear time-varying systems," *Automatica*, vol. 54, pp. 16–24, 2015.

[38] J. Ghommam, H. Mehrjerdi, and M. Saad, "Robust formation control without velocity measurement of the leader robot," *Control Engineering Practice*, vol. 21, no. 8, pp. 1143–1156, 2013.

[39] M. Chen, S. S. Ge, and B. Ren, "Adaptive tracking control of uncertain MIMO nonlinear systems with input constraints," *Automatica*, vol. 47, no. 3, pp. 452–465, 2011.

[40] K. D. Do and J. Pan, "Nonlinear control of an active heave compensation system," *Ocean Engineering*, vol. 35, no. 5–6, pp. 558–571, 2008.

[41] M. Breivik and T. I. Fossen, "Applying missile guidance concept to motion control of marine craft," in *Proceedings of the 7th IFAC CAMS*, Bol, Croatia, 2007.

[42] I. A. Raptis, K. P. Valavanis, and W. A. Moreno, "A novel nonlinear backstepping controller design for helicopters using the rotation matrix," *IEEE Transactions on Control Systems Technology*, vol. 19, no. 2, pp. 465–473, 2011.

[43] A. Levant, "Quasi-continuous high-order sliding-mode controllers," *IEEE Transactions on Automatic Control*, vol. 50, no. 11, pp. 1812–1816, 2005.

[44] D. Angeli and E. D. Sontag, "Forward completeness, unboundedness observability, and their Lyapunov characterizations," *Systems & Control Letters*, vol. 38, no. 4–5, pp. 209–217, 1999.